Feasibility of Hydrogen Energy in Multi End-use Setting in Buildings

Rana Khaled Mohammed Mohammed Saleh

Submitted to the
Institute of Graduate Studies and Research
in partial fulfillment of the requirements for the degree of

Master of Science
in
Mechanical Engineering

Eastern Mediterranean University
August 2022
Gazimağusa, North Cyprus

Approval of the Institute of Graduate Studies and Research

Prof. Dr. Ali Hakan Ulusoy
Director

I certify that this thesis satisfies all the requirements as a thesis for the degree of Master of Science in Mechanical Engineering.

Assoc. Prof. Dr. Murat Özdenefe
Chair, Department of Mechanical Engineering

We certify that we have read this thesis and that in our opinion it is fully adequate in scope and quality as a thesis for the degree of Master of Science in Mechanical Engineering.

Prof. Dr. Uğur Atikol
Supervisor

Examining Committee

1. Prof. Dr. Uğur Atikol
2. Prof. Dr. Mustafa Dağbaşı
3. Assoc. Prof. Dr. Devrim Aydın

ABSTRACT

In the present study, an investigation is conducted to assess the feasibility of producing hydrogen from water and storing it to be used later for electricity generation in a fuel cell. For this reason, it is assumed that a group of hotels that already own a reverse osmosis (RO) desalination unit and an installed 5-MW photovoltaic (PV) system, form a cooperative and share the usage of the hydrogen system. The sales of the byproduct oxygen is also of consideration in the viability study. Hydrogen is generated throughout the year under two scenarios; In the winter period where off-peak electricity is used, and in the remaining seasons where daytime photovoltaic electricity in the grid is used for water splitting by electrolysis to obtain hydrogen. In both scenarios hydrogen is stored during off-peak hours and electricity is generated in a fuel cell during peak hours in North Cyprus. Through the economic analysis, it has been noticed that the system is non-feasible under the current tariff billing. However, using optimization methods through sensitivity analysis and applying Monte Carlo simulation, together with proposing a multi-tariff billing system, it has been observed that the system can become feasible. Through optimization, the fuel cell energetic and exergetic efficiencies are increased to 50.19% and 48.09%, respectively. It is found that the break-even peak and off-peak tariff prices should be 0.55 and 0.275 $/kWh, respectively, with expected reduction in fuel cell and storage unit costs in the future, to obtain savings-to-investment ratios above unity. The analysis was done over a lifetime of 15 years and discount rate of 2%.

Keywords: energy storage, hydrogen energy, economic feasibility, demand curve, sensitivity analysis, Monte Carlo

ÖZ

Bu çalışmada, sudan hidrojen üretip depolamak suretiyle bir yakıt hücresi vasıtasıyla elektrik üretiminin fizibilitesini değerlendirmek için bir araştırma yapılmıştır. Bu nedenle, denize yakın bir otel gurubunun halihazırda bir ters ozmoz (RO) suyu tuzdan arındırma ünitesine ve kurulu 5 MW'lık bir fotovoltaik (PV) sistemine sahip olduğu, bir kooperatif oluşturduğu ve hidrojen sisteminin kullanımını paylaştığı varsayılmaktadır. Yan ürün oksijenin satışı da fizibilite çalışmasında dikkate alınmıştır. Hidrojen yıl boyunca iki senaryo altında üretilir; Kış döneminde elektriğin yoğun kullanılmadığı saatlerde ve diğer mevsimlerde, fotovoltaiklerin elektrik ürettiği gündüz saatlerinde elektroliz yoluyla arıtılmış suyu bölerek elde edilir. Her iki senaryoda da Kuzey Kıbrıs'ta yoğun olmayan saatlerde hidrojen depolanır ve yoğun saatlerde bir yakıt hücresinde elektrik üretilir. Sistemin mevcut tarife ile uygulanabilir olmadığı yapılan ekonomik analizde ortaya çıkmıştır. Ancak duyarlılık analizi ile optimizasyon yöntemlerinin kullanılması ve Monte Carlo simülasyonunun uygulanması, çok tarifeli faturalandırma sisteminin önerilmesiyle birlikte sistemin uygulanabilir hale gelebileceği gözlemlenmiştir. Optimizasyon sayesinde, yakıt hücresi enerjik ve ekserjetik verimlilikleri sırasıyla %50.19 ve %48.09'a yükseltildi. Fizibilitede başabaş gitmek için, gelecekte beklenen yakıt hücresi ve depolama fiyatlarının düşmesi yanında, yoğun ve yoğun olmayan saatlerdeki elektrik fiyatının sırasıyla 0.8 ve 0.4 $/kWh olması gerektiği bulunmuştur. Analiz, 15 yıllık bir ömür ve %2 iskonto oranı üzerinden yapılmıştır.

Anahtar Kelimeler: enerji depolama, hidrojen enerjisi, ekonomik fizibilite, talep eğrisi, duyarlılık analizi, Monte Carlo

DEDICATION

I am dedicating my work to the children of the future.

ACKNOWLEDGMENT

I would like to acknowledge the support of a few people in my life. Starting with my mother and her endless support and motivation and Prof. Dr. Ugur Atikol for his patience and knowledge.

TABLE OF CONTENTS

LIST OF TABLES

LIST OF FIGURES

LIST OF SYMBOLS AND ABBREVIATIONS

c_p	Specific Heat at Constant Pressure
HHV	Higher Heating Value
HS	Hydrogen Storage
I	Current
k	Specific Heat Ratio
LHV	Lower Heating Value
$\dot{n}$	Molar Flow Rate
N_{cells}	Number of Cells
P	Pressure
PV	Photovoltaic
r_{HL}	Heat Loss Ratio
T	Temperature
T_0	Dead State Temperature
T_{opt}	Operating Temperature
V	Voltage
$\dot{W}_{out}$	Rate of Output Work
$\dot{W}_{rev}$	Rate of Reversible Work
X	Exergy
$\dot{X}_{dest}$	Rate of Exergy Destruction
η_I	First Law Efficiency
η_{II}	Second Law Efficiency
η_{ez}	Electrolyzer Efficiency

η_{FC}	Fuel Cell Efficiency
λ	Air Stoichiometry
ψ	Exergy of a Flow

Chapter 1

INTRODUCTION

As global energy demand increases, greenhouse emissions increase and fossil fuel resources decrease. Fossil fuels provide 80% of world's current energy, however air pollution has become a significant issue [1–5]. Thus, the need to produce clean energy to match the demand and protect the environment is emerging. Renewable energy penetration into the grid as an energy source has decreased the share of fossil fuels, reducing CO_2 emissions. However, this has increased grid decentralization with the high penetration of intermittent renewable energy sources. This has caused difficulty in stabilizing the power grid, due to imbalance in supply and demand. Therefore, there is a need to balance the energy supplied from the grid and the energy actually used through storing the excess energy [6–8]. Many scientists are exploring methods of energy generation that preserve fossil fuels and suppress greenhouse emissions.

The present research focuses on hydrogen energy economic utilization for storage and energy generation to preserve fossil fuels and avoid electricity demand peaks. Hydrogen is not only widely abundant, but it also carries the highest energy density compared to other burning fuels[9,10], as shown in Table 1.

Table 1: Gravimetric energy density in kWh/kg of different fuels

Fuel Type	Energy Density (kWh/kg)	Reference(s)
Coal	6.67	[11]
Crude Oil	12.22	[11]
Diesel	12.50	[11]
Gasoline	12.78	[11]
Natural Gas	15.28	[11]
Hydrogen	39.42	[9]

Due to the abundance of hydrogen, it is easily accessible, it is found in and can be produced from natural gas, water, coal, and biomass [12]. However, the extraction of hydrogen from compounds other than water produces CO and CO_2 as byproducts [12,13]. Therefore, water electrolysis (shown in Figure 1), which is the production of hydrogen by using electricity to split water molecules, is the cleanest option. The overall reaction is $H_2O \rightarrow H_2 + \frac{1}{2}O_2$ [13].

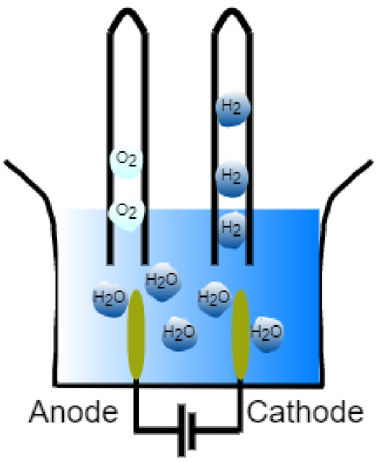

Figure 1: Water electrolysis

According to World Economic Forum; Climate Action, hydrogen production can be categorized into four color-assigned categories depending on the source and the gas produced, as shown in Table 2 [10]. Green hydrogen production is when the products of the process do not include toxic gases. Compared with gray and blue hydrogen production, green hydrogen production releases oxygen as its only byproduct via water electrolysis. In green hydrogen production, water electrolysis is carried out by renewable energy source.

Table 2: Categories of hydrogen production [10]

Color	**Black/Brown/ Gray**	**Blue**	**Green**
Source	Methane or coal	Methane or coal	Water
Methods	Steam reformation or gasification	Steam reformation or gasification with carbon capture	Electrolysis (renewable electricity)
Byproduct	Carbon dioxide and carbon monoxide	Underground (trapped) carbon dioxide	Oxygen

Moreover, he demand curve is essential as it shows the electrical energy requirement for a region at different times. Shown in Figure 2 is the hourly demand in megawatts during summer in North Cyprus. Proceeding with electricity generation, a valley occurs in the energy demand graph, as shown in Figure 2, at the times of low demand.

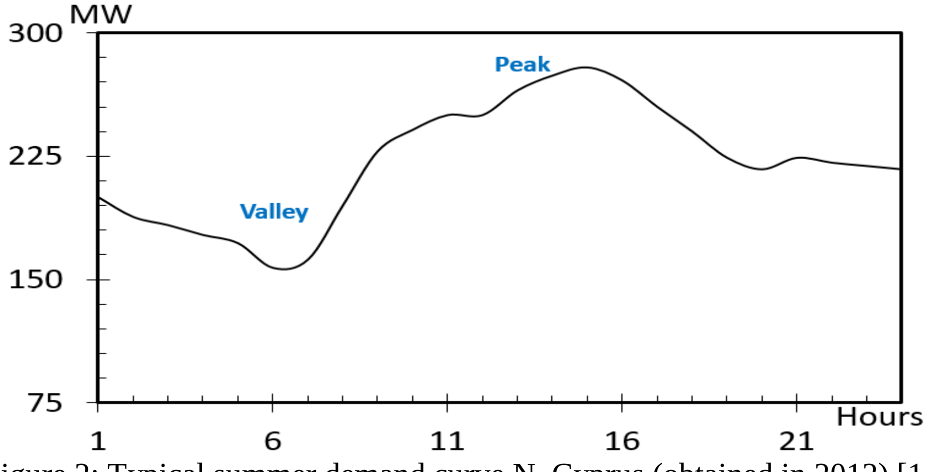

Figure 2: Typical summer demand curve N. Cyprus (obtained in 2012) [14]

Solar energy is considered a renewable energy source that does not emit CO_2. Therefore, it has become a clean alternative to electricity production. However, it still cannot replace the conventional power plant due to its low efficiency and intermittency. In North Cyprus, the sun shines between 06:00a.m. and 08:00p.m., in the best case, where it can be hindered by intermittency and discontinuity, as shown in Figure 3. Solar penetration into the grid has been increasing, creating a problem visualized as the "duck curve", shown in Figure 4. The duck curve occurs due to the fact that peak solar production happens midday, as demonstrated in Figure 2 [15]. Therefore, the energy produced by the conventional power plant drops and the net demand falls. The net demand is the integrated wind and/or solar production minus the total demand. On the other hand, as net demand starts to increase, approaching the evening, solar power generation drops. This creates a problem as power utilities supply more power as they ramp up to match the high demand. Utility ramps up production to compensate for this gap, overstressing, and possibly damaging the grid that is not yet equipped for these peaks. The Cyprus duck curve is expected to worsen as more solar energy is penetrating the grid.

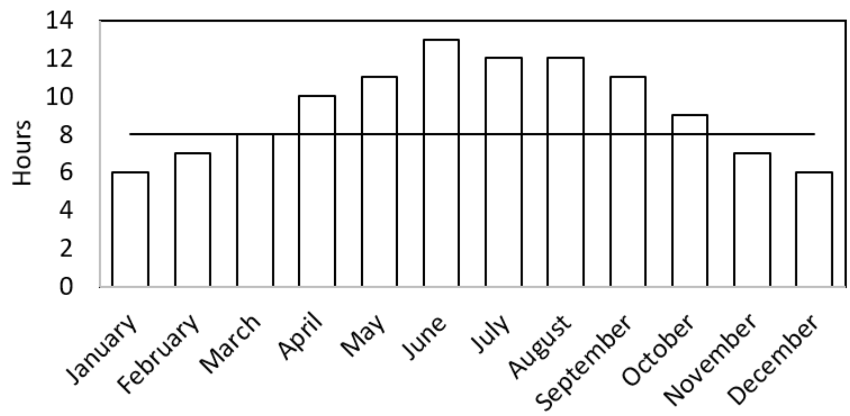

Figure 3: Daily average sunshine duration by month in Nicosia [22]

To flatten the duck curve, storing the solar energy becomes a solution to the duck curve. The stored power can be later utilized during the peak periods. This solves two main issues;

- Solar power is not wasted.
- Power grid overloading is avoided.

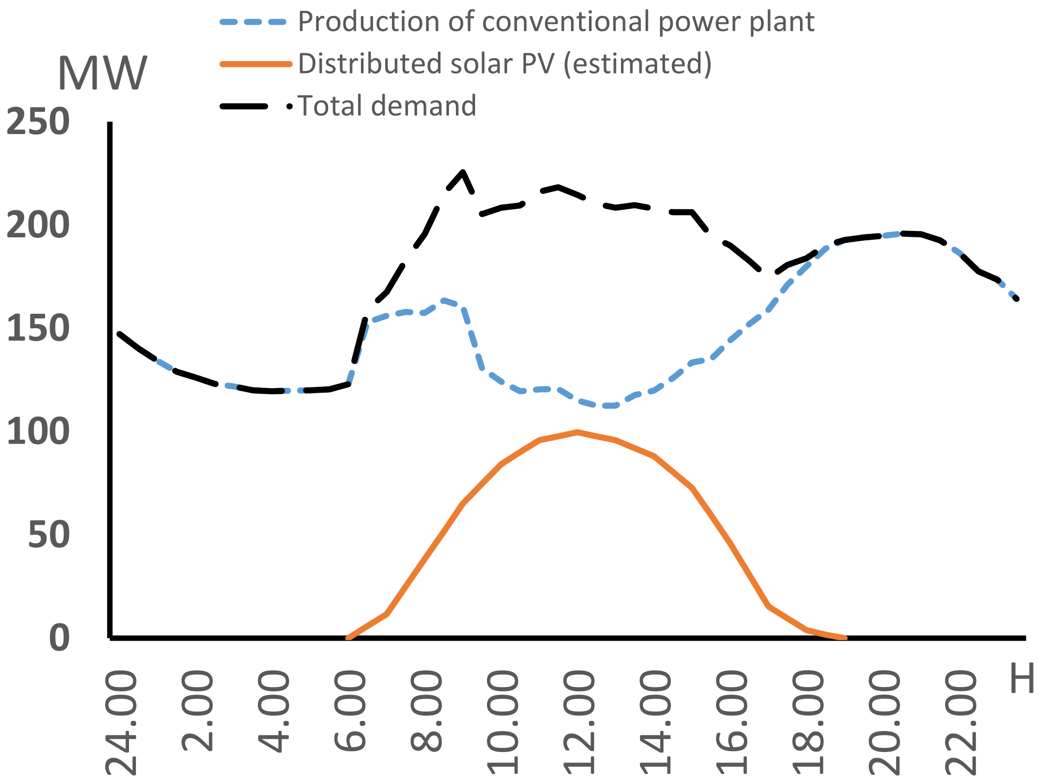

Figure 4: Cyprus duck curve with estimated solar power (March 16, 2022)

To further reduce the environmental impact of conventional energy generation, hydrogen storage can be utilized. This is an approach that integrates electrolysis, using a device called an electrolyzer, and an electrochemical power conversion from the produced hydrogen [16]. Power regenerated from chemical sources like hydrogen undergo a process where hydrogen reacts with oxygen to generate electricity, heat and water. This electrochemical reaction is completed in a device called a fuel cell [17]. To avoid high peaks in the demand curve, the fuel cell converts the stored H_2 to electrical energy [16,18,19]. Furthermore, electrolysis consumes 39.4 kWh to produce 1 kgH_2 [16]. Thus, to satisfy the energy demand during the peak hours, a multi-tariff system can be proposed instead of the current constant rate billing where off-peak hours are utilized to produce hydrogen, in one case, and solar energy is consumed to produce H_2 through an electric cooperative, in another case. An electric cooperative can be established for significant solar energy consumption. An electric cooperative is a private, non-profit establishment that distributes electricity to its members and owners in the service area [20,21]. It is an alternative to commercial utility companies and all its members have equal status. There are two types of an electric co-op, distribution co-op and generation and transmission co-op (G&T)[20,21]. In a distribution co-op, it is organized that the members are directly supplying and consuming the electricity [21].

However, solar energy is not continuously available throughout the year. For example, during winter the solar availability drops to 6 hours compared to summer, fall, and spring which is averaged to 11.5 hours, as shown Figure 3 [22].

Henceforth, two scenarios can be implemented; (a) a winter scenario utilizing multi-tariff billing and (b) a summer scenario utilizing solar PV for H_2 production. The peak hours, shown in Figure 5, are approximately between 05:00 p.m. and 9:00 p.m. Therefore, in a multi-tariff electricity billing, the off-peak tariff is cheaper than the peak tariff [14]. Consequently, the consumer could use the produced hydrogen for electricity during the expensive peak hours.

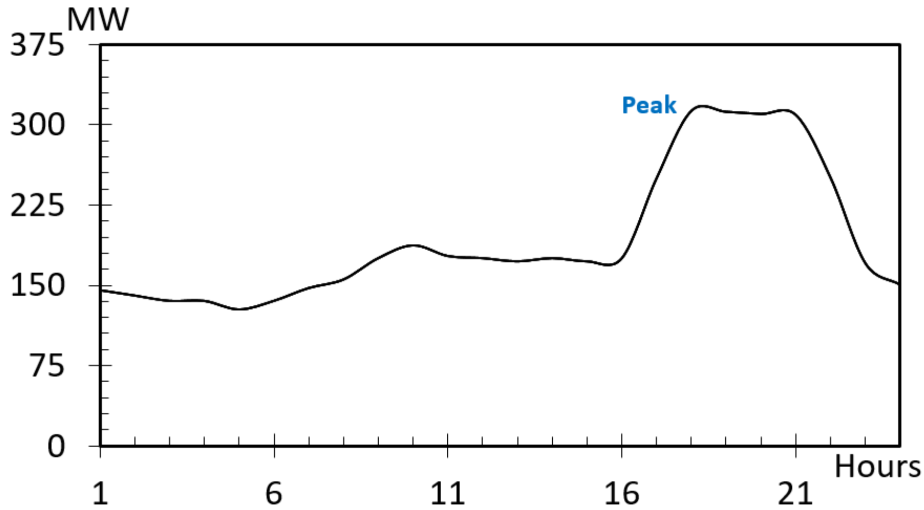

Figure 5: Typical winter demand curve N. Cyprus (obtained in 2012)[14]

It is clear that energy storage becomes essential in N. Cyprus and green hydrogen, being a clean option, can be considered. However, the cost of hydrogen production is high and poses a threat to its large-scale utilization[13,19,24,25]. Also, presently, the low fuel cell efficiencies, ranging from 40% to 50%, affect the total system's efficiency [18,26,27]. Thus, it negatively impacts the economic feasibility.

Application of green hydrogen projects make more sense as they can be made into multi-generation units and are more likely to be feasible. For this reason, large-scale applications in industrial and commercial sectors can be considered. In the current study, it is aimed at investigating the possibility of setting up a 15-MWh green hydrogen storage system owned by several hotels in a hotels region, such as the one in Bafra, N. Cyprus. These hotels can set up an energy cooperative to manage such a system. In hotels region, like the one in Bafra, there is a possibility of utilizing the existing large scale solar photovoltaic (PV) panels through an electric cooperative, where all the hotels are owners and consumers. In addition, it can be assumed that there is an existing reverse osmosis (RO) plant that can be used as the water source for electrolysis due to the fact that hotels utilize RO treated water as their source of clean, potable water.

The objective of the present research is to assess the feasibility of (a) utilizing hydrogen storage (HS) using the multi-tariff electric billing in winter and (b) using solar energy for hydrogen production in summer, fall, and spring in a hotels region in North Cyprus. The feasibility analysis will comprise a techno-economic analysis of the critical system parameters for each case to reach optimal results.

The thesis from this point onwards is divided into the following parts;

- In Chapter 2 a literature review combining various research studies of feasibility of hydrogen energy storage, production, and electricity; polymer electrolyte membrane (PEM) electrolyzers and PEM fuel cells (PEMFC); and exergy analysis of PEMFC.
- In Chapter 3 a description of the system and proposed scenarios.
- In chapter 4 the methodology followed for economic feasibility with thermodynamic analysis and optimization methods.
- In Chapter 5 elaborated results and discussion on the simulation.
- In Chapter 6 a concise and succinct overall conclusion based on results, method, and simulation.

Chapter 2

LITERATURE REVIEW

In this chapter, a literature review of hydrogen storage and production technologies, different fuel cell technologies, an overview of electric cooperative, and comparative study of PEMFC exergy analysis are provided. The aim of literature review is to examine the currently available research and technologies on hydrogen storage.

2.1 Hydrogen energy storage

Chemical energy storage can be obtained when electrical energy is used to produce chemical compounds that can be stored and reused for energy generation. Hydrogen is a chemical that is storable and acts as a clean energy carrier. It can be stored as compressed gas, liquefied gas, and metal hydride [8,13,19,28]. However, hydrogen has lower volumetric energy density than most fuels creating volumetric sizing penalties on hydrogen storage devices, increasing the cost [19]. Volumetric energy density measures the amount of energy that can be contained in a given volume [29]. The selection of hydrogen storage type depends mainly on usage and price.

A review study by Argonne National Laboratory compares costs of different hydrogen storage methods [28,30]. A summary of the comparison is shown in Table 3. Based on the data collected from Table 3, metal hydride is the most expensive hydrogen storage method. Liquid hydrogen storage with capacity of 10.4 kg H_2 is the cheapest hydrogen storage method.

Table 3: Different hydrogen storage systems specifications

Method	**Pressure (bar)**	**Capacity (kg_{H2})**	**Gravimetric density (kWh/kg)** [13]	**Temperature (K)**	**Total cost ($/kWh)**	**Source**
Compressed hydrogen	350	5.6	1.8	-	16.1	Law 2013[30]
	700	5.6	1.5	-	19.6	Law 2013[30]
Liquid hydrogen	-	5.6	-	-	10	Law 2013[30]
	-	10.4	-	-	5	Law 2013[30]
Cryo-compressed hydrogen	275.6	5.6	-	<100	15.1	Law 2013[30]
	275.6	10.4	-	<100	10.6	Law 2013[30]
Metal hydride	-	0.036	0.4	-	2918	Argonne[28]

However, liquid hydrogen is stored in cryogenic containers that requires insulation of multiple layers of reflective heat shields between the walls of the vessels, and requires a liquefaction plant [28]. Keeping the liquid hydrogen at cryogenic temperature can be difficult to maintain due to the boil-of phenomenon that reduces the efficiency, the insulation components increase the weight of the storage system, and hydrogen has to be cooled to 21 K for liquefaction, where it loses 30% of its lower heating value [13].

Therefore, compressed hydrogen becomes the most suitable option for the present research. According to the U.S. DOE, 700 bar compressed hydrogen storage and 350 bar compressed hydrogen storage unit cost are 12 $/kWh and 8 $/kWh as of 2014, respectively [31].

Table 4: Volumetric energy density in MJ/L for different fuels [19]

Fuel	**Volumetric energy density (MJ/L)**
$Hydrogen_l$	10.1
$Hydrogen_g$ (700 bar)	5.6
$Hydrogen_g$ (1 bar)	0.0107
Methane (1 bar)	0.0378
Natural gas_l	22.2
Natural gas_g (250 bar)	9
Gasoline (petrol)	34.2
Diesel	34.6

Another study confirms that hydrogen energy storage (HES) in renewable energy applications is viable with long time scale and efficiencies ranging between 65-75%. HES satisfies fluctuations and spikes in energy demand, as well as forms a bridge filling the gaps between electricity outages [32].

2.2 Electrolysis

The device that conducts the electrolysis process is called an electrolyzer. An electrolyzer breaks down the bond between hydrogen and oxygen molecules in water. Water is pumped at the anode, and the covalent bond between the hydrogen molecule and oxygen is broken as electricity is supplied to the electrolyzer. The hydrogen ions, carrying a positive charge, separate from oxygen at the membrane, and the oxygen is released to the atmosphere through the anode (the positively charged port). The hydrogen passes through the membrane and exists the electrolyzer through the cathode (the negatively charged port), as shown in Figure 6 [24,33,34]. PEM electrolyzers (PEME) utilize a solid polymer electrolyte that is titanium or platinum coated titanium, Iridium as catalyst material on the anode, and carbon paper or carbon fleece at the cathode [35].

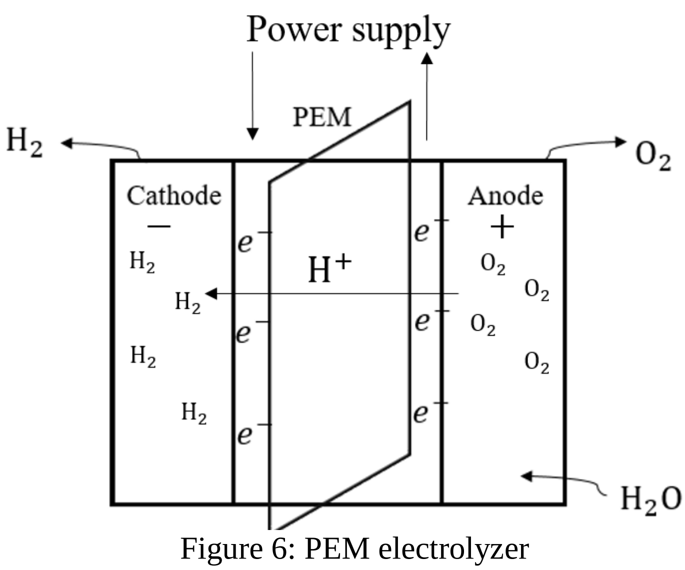

Figure 6: PEM electrolyzer

Today, China is the largest producer of hydrogen, where 95% is derived from fossil fuels [36]. This correlates with the global hydrogen production share by a source [23] in a 2008 study, shown in Table 5.

Table 5: Global hydrogen production share by source based on a 2008 study

Source	**Percentage share**	**References**
Natural gas	48	[19,37]
Oil	30	[19,25,37]
Coal	18	[19,25,37]
Electrolysis	4	[19,37]

Different water electrolysis technologies include alkaline water electrolysis, proton exchange membrane water electrolysis, solid oxide water electrolysis, and alkaline anion exchange membrane water electrolysis. Alkaline water electrolysis (AWE) operates at low temperatures with an aqueous solution as the electrolyte, which creates an alkaline fog in the generated gas. Proton exchange membrane water electrolysis (PWE) uses protons in the membrane, making it more environmentally friendly [26,36,38].

A comparison between alkaline water electrolysis and PEM water electrolysis is shown in Table 6 [36,38,39]. Based on Table 6, PWE shows great promise due to it being environmentally friendly, having high efficiency, and rapid start-up. The rapid start-up allows it to handle the intermittency of renewable energy power supply. According to U.S. National Renewable Energy Laboratory, PEM electrolysis is evaluated as a suitable technology for converting wind power into hydrogen generation [36,40].

Table 6: Alkaline and polymer exchange water electrolysis comparison [36,38,39]

	AWE	PWE
Membrane	Porous asbestos	Proton exchange (polymeric)
Environmental	x	✓
Efficiency	59-70%	65-82%
Risk(s)	• Explosion due to asbestos membrane • Corrosive electrolyte • Gas permeation	-
Start-up	Long	Rapid
Advantages	• Relatively stable • Low capital cost	• Compact design • Fast response • High hydrogen purity

It is also expected that the PWE cost will decrease to quarter of its current price by 2025 [36]. Unlike AWE, PWE does not requires a compressor for high pressure, leading to a possible reduction in capital and operating costs [26]. Furthermore, AWE electrolyzer uses basic solutions, such as NaOH as electrolytes to expedite the electrolysis process, using less power. However, basic solutions are highly corrosive, which limits the material of the electrodes to nickel, cadmium, and other corrosion resistant materials. These materials are not abundant and require excavations to be obtained, which deems the AWE as a non-renewable electrolysis process [8]. Also, according to U.S. DOE, varying electricity costs affect hydrogen production cost, where it is estimated to reach 4-5 $/kg for forecourt and central size plants at an average cost of electricity of 6.12-6.89 ¢/kWh [38].

The assumed purity of the outlet hydrogen is 99.999%, according to references [13,33,41]. Pure deionized water is used in the electrolysis process, according to Nel Hydrogen [42]. However, the water lacks ions, not allowing it to carry enough charge, thus an electrolyte is utilized to facilitate the electrolysis process [35]. While seawater is considered the best type for electrolysis, it is short-term based [43]. It is challenged by high cost and damaging chlorine in its chemical structure [44].

Therefore, reverse osmosis (RO) is required to deionize and desalinate the available sea water source. According to Atikol & Hikmet [45], RO is considered the most feasible desalination technology that produces fresh water. The estimated unit cost of freshwater produced is 0.7$/m^3 [45].

2.3 Power conversion

A fuel cell is an electrochemical device by which electrical energy is produced through combining hydrogen and oxygen and releasing water into the atmosphere [19,46–51]. Currently, the most commonly used fuel cell technology is polymer electrolyte membrane (PEM) due to its low operation temperature, high efficiency and power density, and convenient stacking for stationary power generation application [52]. In a hydrogen fuel cell, the catalyst at the anode separates hydrogen molecules into protons and electrons which are transported in different paths to the cathode. The protons pass through the electrolyte to the cathode and unite with oxygen. The electrons pass through an external circuit creating an electricity flow and combining with the oxygen to produce water and heat [48–51].

The final stage of the hydrogen cycle is the energy conversion technology used. Hydrogen can be directly used as a fuel in an internal combustion engine or a hybrid internal combustion engine-fuel cell. In fuel cells, hydrogen reacts directly with air, unlike in an internal combustion engine, it is burned directly instead of a fossil fuel without the need to compress or spark-ignite it. Fuel cell convert chemical stored energy in hydrogen to DC electric energy. A fuel cell stack is a series of combined individual cells. Solid oxide fuel cells (SOFC) and polymer electrolyte membrane fuel cells (PEMFC) are considered the two main fuel cell technologies in the hydrogen economy. However, SOFC's have maximum theoretical efficiencies that can exceed 80% and PEMFC's have maximum theoretical efficiencies up to 68% [19,53,54].

Table 7: Comparative research between SOFC and PEMFC

SOFC	**PEMFC**
Protective coating required, otherwise rapid performance deterioration [55,56]	Polymer electrolyte membrane which acts as fuel cell electrolyte[57]
Cathode poisoning by chromium from vaporization, causing performance deterioration and environmental risk [55,58,59]	Lower operating temperature [60,61]
Efficiencies between 45-65% [60]	Polymer electrolyte reduces possibility of corrosion [57]
Variety of catalysts [60,61]	Improvements to work with ambient pressure and high temperature [61]
High operating temperature [60,61]	Simpler design [60,61]
Longer durability [60,61]	Lighter weight [60,61]

According to Table 7, SOFC poses higher risk to environment and users due to the cathode poisoning, in addition to being more expensive [53]. And although improvement research to avoid the performance deterioration is in progress, PEMFC is currently the safer option.

2.4 Electric cooperative

In the late 1990s, electric restructuring took place that aimed to introduce a wholesale market competition and served as a major regulatory reform. Fifteen states in the U.S.

implemented market pricing, where a considerable number of generation plants converted to non-utility generation companies operating at a level not regulated by the state. Majority of the power generation plants that remained unchanged were the renewable plants, cooperative owned plants, and plants that were retained due to social geographic considerations [62]. Since the restructuring era, the distribution markets and cooperatives remained significantly unvaried [63]. According to Jang [63], firms with G&T ownership have 6% higher productivity. Also, according to Greer [64], distribution cooperative mergers between firms can help achieve substantial savings and ensure survival.

2.5 Thermodynamic analysis of PEMFCs

Exergy analysis is an important thermodynamic tool for developing, evaluating, and improving energy conversion systems. Exergy analysis offers an approach to true ideality of a system through exergy efficiencies. It assesses the performance of an energy system. Exergy methods clearly identify the causes of exergy losses, allows for economic and environmental improvements, and helps in optimization [65].

Multiple case study exergy analyses on PEM fuel cells are present in the literature. They examine the effect of varying operating conditions, including temperature, pressure, air stoichiometry, and current densities [66–69].

The data illustrated in Figure 7 show different research results and conclusions on exergetic and energetic efficiencies. However, two conclusions apply to all the case studies; exergetic and energetic efficiencies (η_{en} and η_{ex}) increase with increasing operating temperature and pressure (T_{opt} and P_{opt}); and exergetic and energetic efficiencies decrease with increasing current density (J) [66–69]. The model generated by Baschuk and Li (2003) concludes that output power ($\dot{W}_{out}$) increases with increasing pressure (P) [69]. Compared with the 1.2 kW PEMFC, where the output power ($\dot{W}_{out}$) increases with the current density (*J*) [66]. However, the 5.75 W PEMFC shows that significant increase in the power output ($\dot{W}_{out}$) occurs with the increasing number of cells (N_{cells}) [67].

The current work will look into optimizing parameters such as number of cells, operating temperature, and air stoichiometry in order to achieve higher energy and exergy efficiencies for a 1000-kW Nedstack fuel cell.

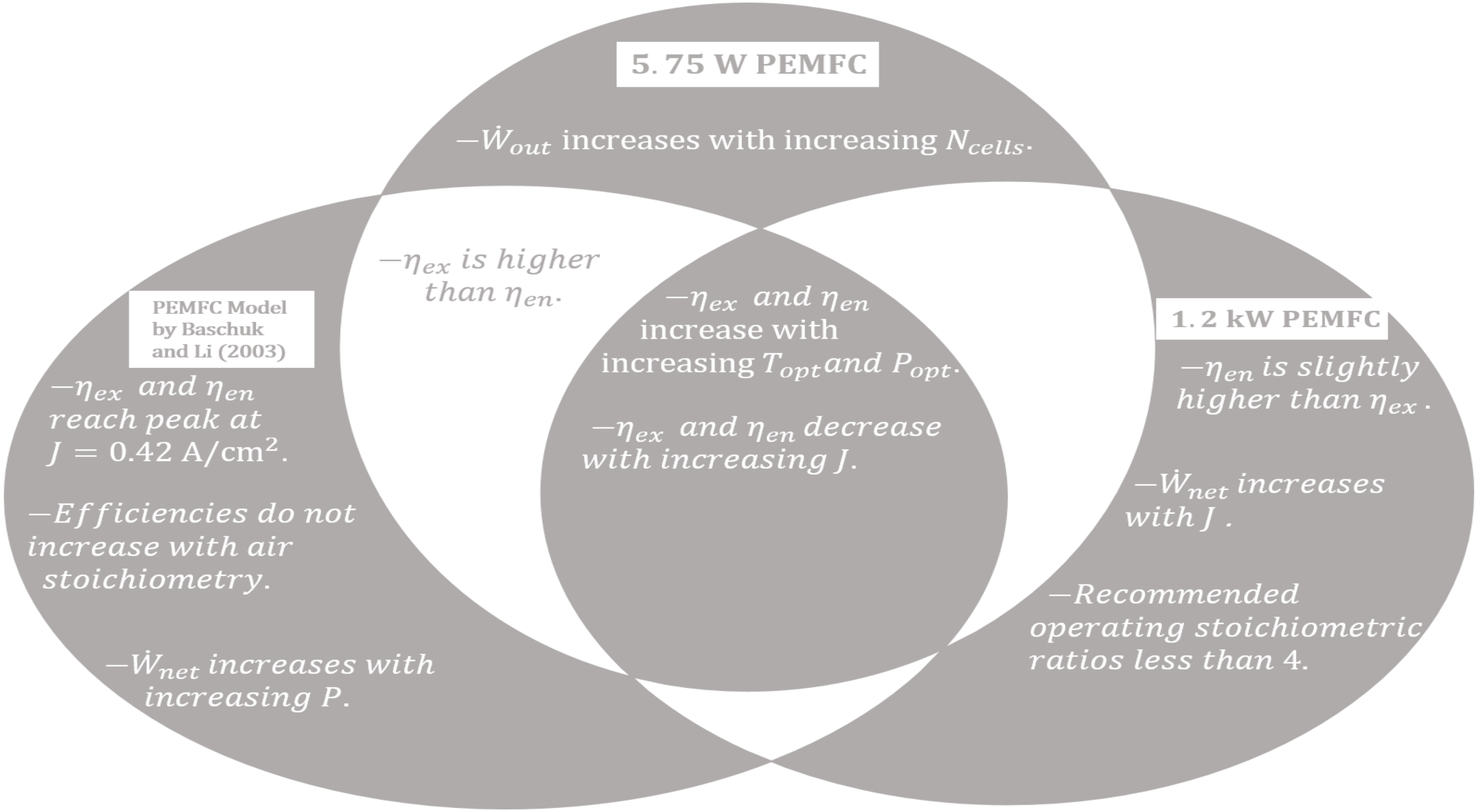

Figure 7: Comparative review of exergy analysis on different PEMFCs[66–69]

Chapter 3

FEASIBILITY AND OPTIMIZATION

Two different scenarios for hydrogen storage are studied in the present research; (a) a winter scenario utilizing off-peak electricity via multi-tariff electricity billing system, and (b) a summer scenario utilizing solar energy. The system produces hydrogen through electrolysis, where R.O treated water passes through the electrolyzer. The hydrogen produced is stored for later usage during high demand periods. Hydrogen can be stored in tanks as compressed gas or liquefied for long periods ranging between 20 to 30 years [32, 69]. When the energy demand rises, an electrochemical reaction occurs as hydrogen flows from the storage tanks to a device called fuel cell. In the fuel cell, hydrogen molecules combine with oxygen molecules generating electricity [48]. Figure 8 represents the integration of electrolysis, hydrogen storage, and fuel cell electricity production.

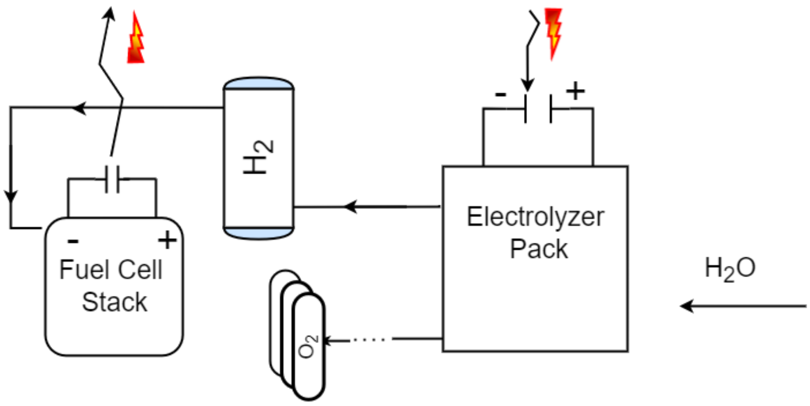

Figure 8: Integrated fuel cell and electrolyzer process diagram

3.1 Hydrogen storage

Storing energy is a way of energy management and reducing energy costs for utility plant and end-users, by smoothing the energy demand profile and investigating alternative low-rate methods of producing and purchasing energy [47]. As shown in Figure 9, the demand curve has a noticeable low demand profile in the early morning during which the electricity tariff is at its cheapest as shown in Table 8. Therefore, hydrogen produced during these hours, which are approximately between 12:00 A.M. and 06:00 A.M., can be stored for when the energy demand spikes again at approximately 05:00 P.M.

Similarly, in summer, although the demand is at its highest during the midday, due to distributed solar energy in the grid there is a sudden increase in the conventional power plant demand in the early evening when the sun sets, as shown in Figure 10 [15]. Hence, the solar energy is required to be stored for usage during the early evening period. An energy production and consumption balance can be attained via strategizing and energy storage, as demonstrated in Figure 9 and Figure 10.

According to Giovanni [47], the application of load management techniques may give economic benefits to utility rates, which can be achieved by reducing the peaks without sacrificing power production quality and quantity.

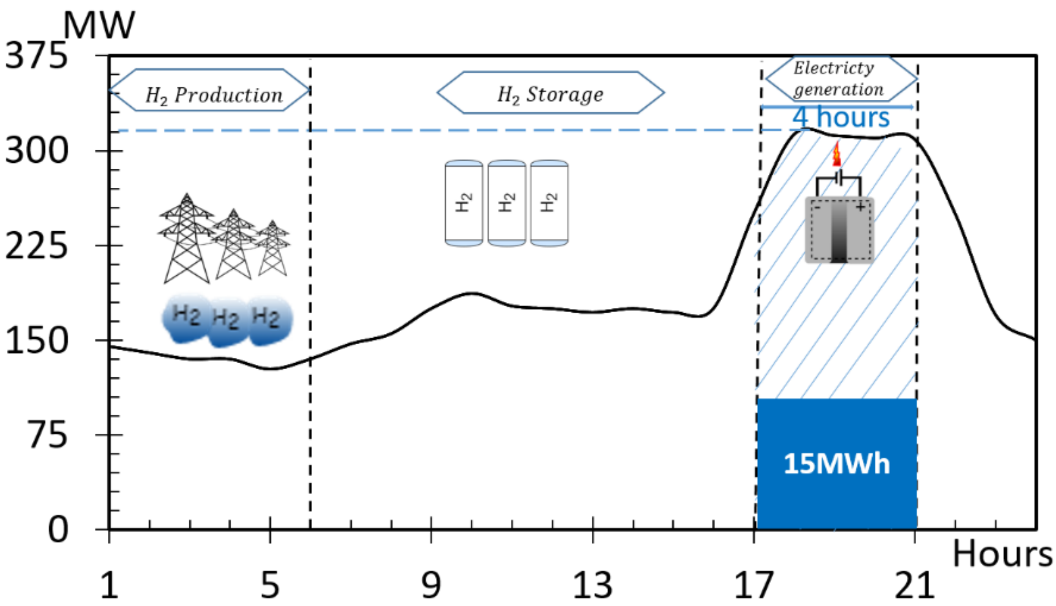

Figure 9: Scenario description on winter energy demand curve

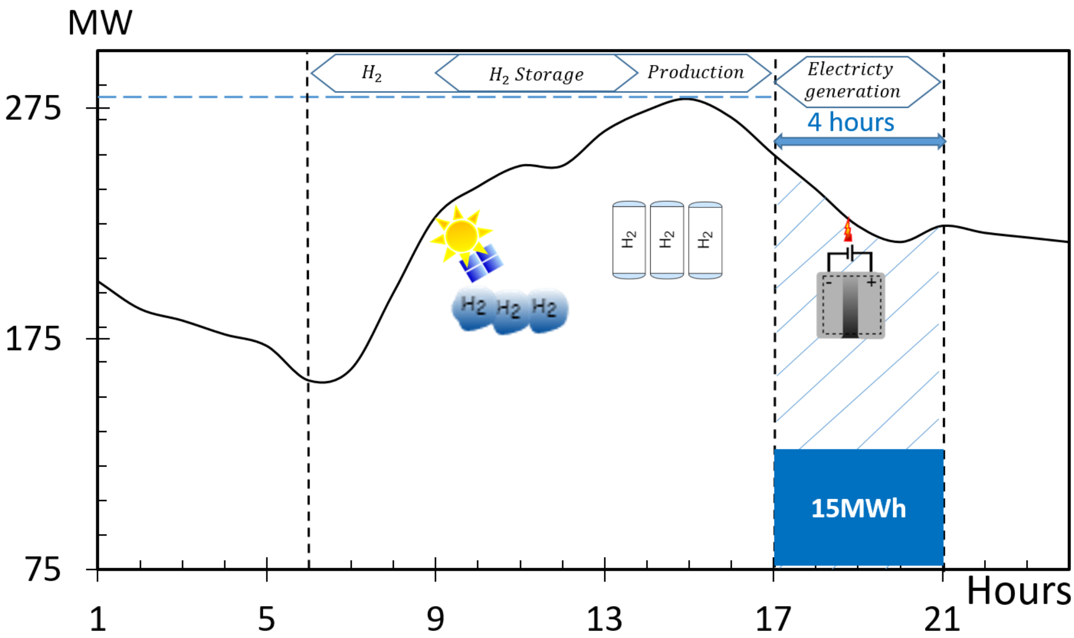

Figure 10: Scenario description on summer energy demand curve

Figure 11 shows the proposed transfer of current energy generation methods. The transfer is based on energy strategies via implementing energy storage.

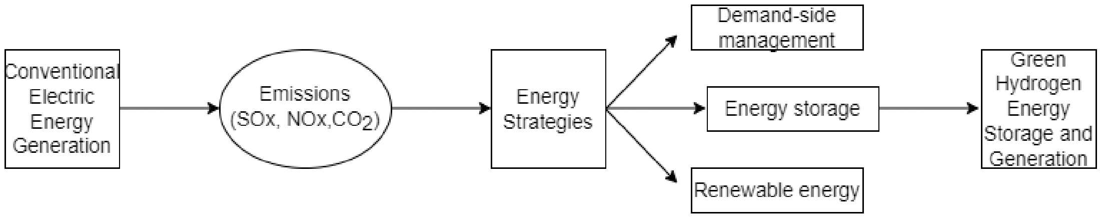

Figure 11: Energy management flowchart

High pressure compressed hydrogen storage is currently widely adopted for stationary, vehicular, and bulk transportation of hydrogen [71]. According to reference [71], high pressure gaseous hydrogen ($HPGH_2$) is mainly used for large-scale application where low-cost hydrogen storage is required. The significant advantages of $HPGH_2$ are technology simplicity and rapid filling and releasing rates. The rapid filling-releasing rate matches ideally with the sudden spikes in the demand. However, it is seen from Table 3 that the gravimetric density decreases as the compressed gaseous hydrogen pressure increases. Gravimetric energy density measures the amount of energy per unit mass. Also known as specific energy [72]. It can also be observed from Table 3 that the unit cost is lower at 350 bar than it is at 700 bar. However, in the present study, a 1,000 kg hydrogen tank at 700 bar will be utilized from NPROXX 2022 manufacturers [73].

Gases travel from high pressure to low pressure areas [74]. This key characteristic of gases allows for the transportation of hydrogen without the need of compressors, as shown in Figure 12. Hydrogen is produced in a PEME at operating temperature of 1000kpa. It then travels to compressed hydrogen storage tank at a pressure of 700kpa. Stored hydrogen is then released into the PEMFC, where the operating temperature is 600kpa.

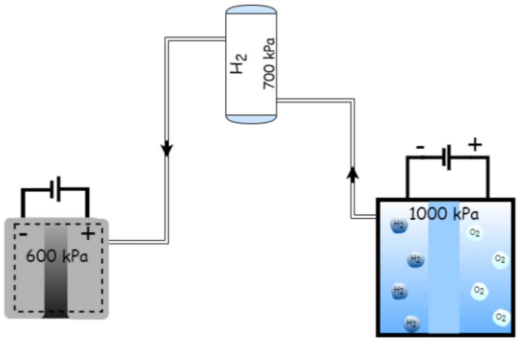

Figure 12: Hydrogen flow

3.2 Winter scenario via multi-tariff electricity billing

The objective of integrating hydrogen storage generation is to reduce the cost of electricity and avoid spikes in the energy demand curve, shown in Figure 2. These spikes or peaks can be reduced when the electricity generated by the fuel cell is used to meet part or all of the demand. This creates a peak shaving, as shown in Figure 13. Furthermore, off-peak hours create valleys in the energy demand curve. These valleys, shown in Figure 2, can be utilized to power the electrolysis process. This is called valley filling. Peak shaving and valley filling are methods of energy management and strategy [75].

According to Kib-tek[1], the winter peak and off-peak hours and prices are shown in Table 8 based on the last implemented multi-tariff prices in 2021. It is proposed that a multi-tariff electricity billing could be implemented instead of liar-based to shift consumers to utilize electricity during the relatively lower demand hours to reduce the peaks.

[1] Kib-tek is the electricity board responsible for power production and distribution in N. Cyprus.

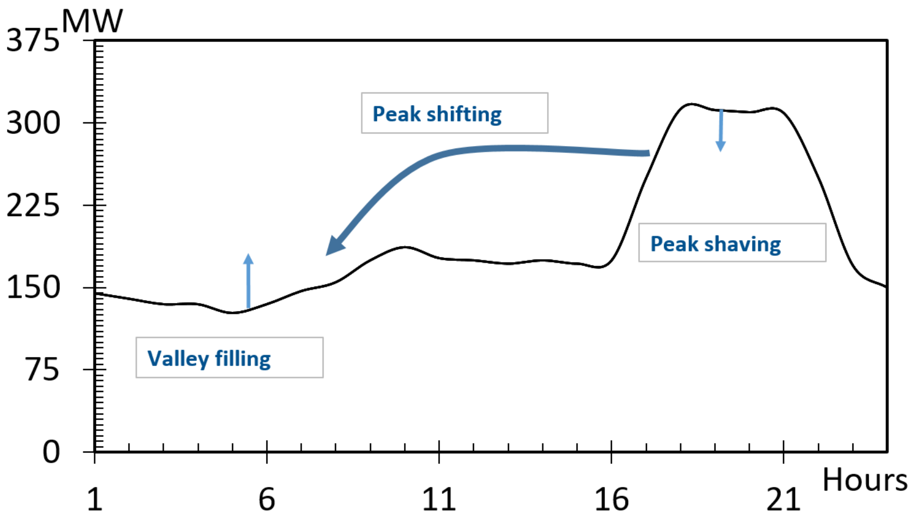

Figure 13: Energy flexibility strategy [75]

Table 8: Electricity tariffs in N. Cyprus (2021) [23]

Electricity prices		
	Off-peak	Peak
Period	24:00-06:00	17:00-21:00
Price ($/kWh)	0.125	0.25

Based on the data collected from Table 8, it can be seen that the off-peak hours are between 12:00 a.m. and 06:00 a.m. and the electricity price is half of the peak tariff. Therefore, this approach is suggested for the winter time of the year, where the solar radiation is low.

During the off-peak hours, electricity is relatively cheap which facilitates its usage to produce hydrogen through electrolysis. Consequently, as the demand increases throughout the day, peaks in the demand occur which last for approximately 4 hours. These periods are called the peak hours. Peak hours consume much more electricity than off-peak periods causing the utility to ramp up production, making the peak tariff more expensive. Therefore, the hydrogen (energy) storage becomes essential. Storing the produced hydrogen allows for electricity generation through an alternative to the thermal power plant. A PEM (polymer electrolyte membrane) fuel cell is used to generate the electricity via converting the chemical hydrogen energy into consumable electric energy, as shown in Figure 14.

3.2.1 Winter scenario operation

Working schedules for PEME and PEMFC depend on the energy management strategy. Since winter scenario is based on multi-tariff electricity prices for hydrogen production, the working schedules will significantly depend on the demand profile. In winter, grid-powered electricity can be used to power the hydrogen production in the off-peak periods. This will create valley filling in the winter demand curve, as shown in Figure 13.

Consequently, the working schedule for winter hydrogen storage can be engineered in a manner where the cheaper off-peak electricity prices are utilized as shown in Table 9.

Table 9: Winter operating schedule

Time period	Process	Comments
12AM-6AM	Hydrogen production	- Relatively low demand. - Cheaper tariff price. - Suitable for hydrogen production.
6AM-5PM	Hydrogen storage	- Suitable for hydrogen storage until peak hours.
5PM-9PM	Hydrogen energy electricity generation	- High energy demand. - Expensive electricity tariff. - Suitable for electricity generation from stored hydrogen.

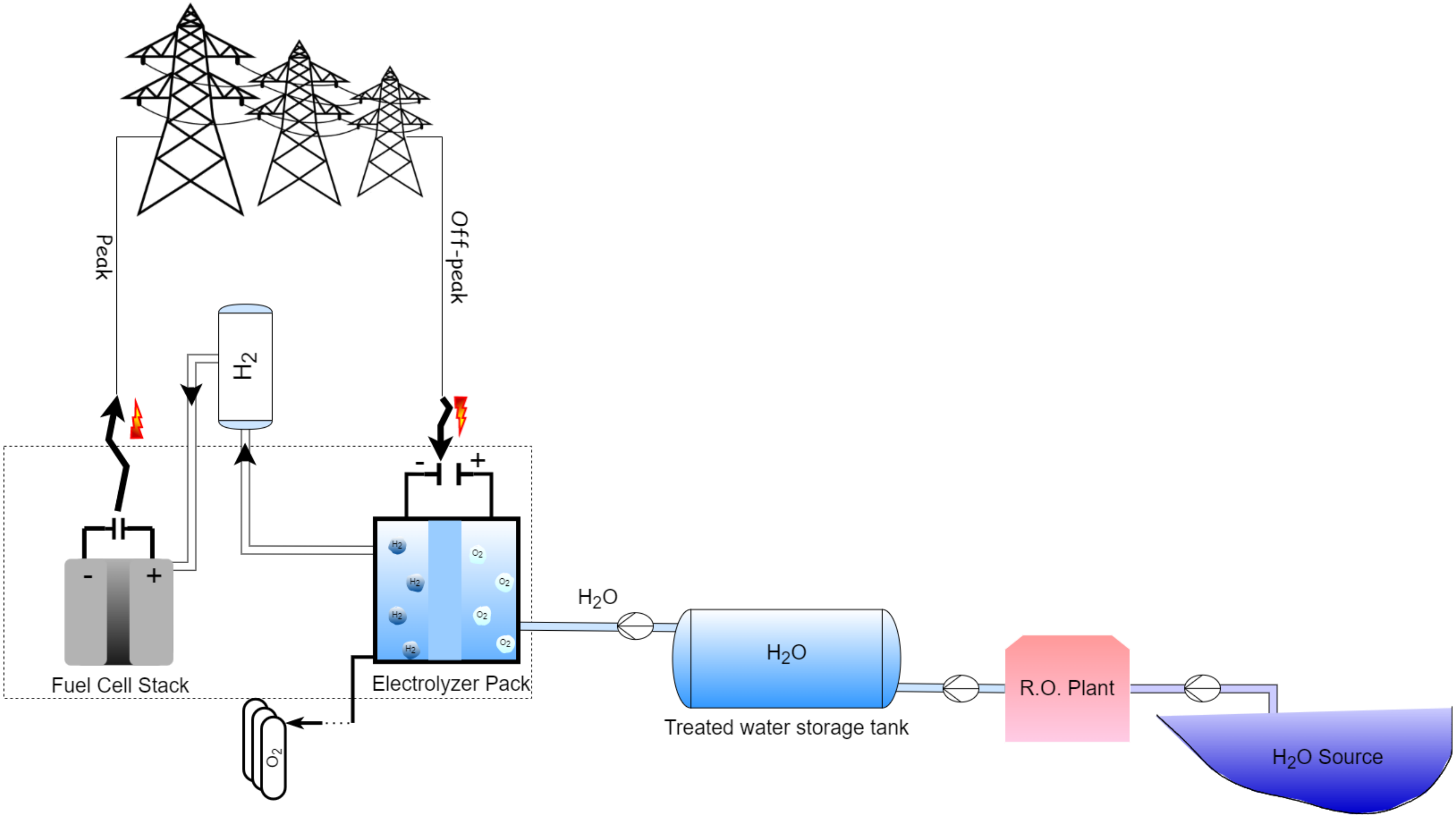

Figure 14: Hydrogen storage under multi-tariff electricity billing

3.3 Summer scenario via PV solar panels

Solar hydrogen energy storage is a type of green hydrogen energy. The system produces hydrogen through electrolysis utilizing solar energy harvested in photovoltaic (PV) solar panels, as shown in Figure 16. Solar energy is a renewable energy source, where one of the most concerning issues is intermittency. Intermittency means that the renewable source is not continuously available [26].

However, PEME's have rapid start-up which allows them to adapt to the intermittency of the solar energy.

In the current research the techno-economic feasibility of the combined winter and summer scenarios with a capacity of 15 MWh in a setting where a group of hotels, such as the one in Bafra region for an electric cooperative. It is assumed that these hotels share a previously built 5 MW solar photovoltaic (PV) panels operated via an electric cooperative, an existing sea water reservoir, an existing reverse osmosis plant, and existing water storage tank(s). The assumptions are summarized in Figure 15.

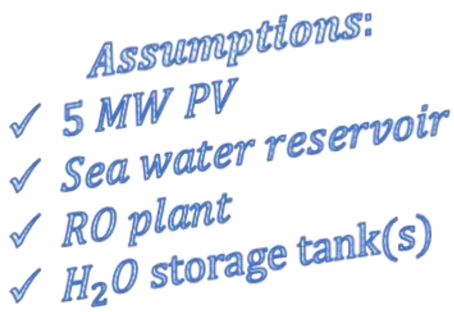

Figure 15: Investigation assumptions

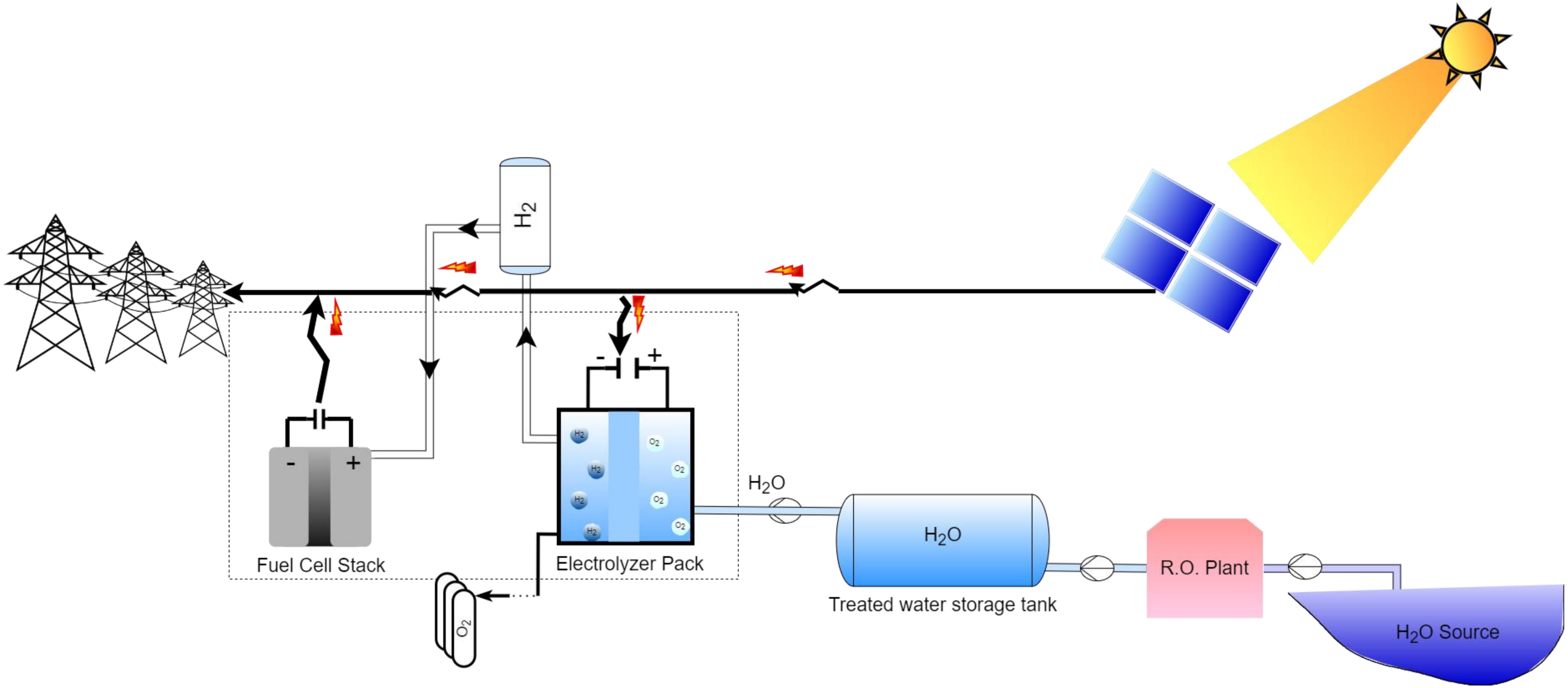

Figure 16: Green hydrogen energy: production, storage, and electricity generation proposed design

3.3.1 Summer scenario operation

Working schedules for PEME and PEMFC depend on the energy management strategy. Since the summer scenario is based on solar hydrogen energy for hydrogen storage the working schedules will significantly depend on the hours of solar availability. In summer, solar intensity is high throughout the day, thus green hydrogen produced from the electrolyzer stack can be utilized later during the peak hours. This lowers the spikes during the peak periods creating peak shaving and allowing for an effective energy production strategy, that relieves the power plant from over-working to meet the sudden spike in demand and reduces toxic emissions into the atmosphere [8].

Summer hours are taken with reference to North Cyprus. According to reference [76], North Cyprus sunrise is approximately 05:35a.m. And sunset is at approximately 08:00p.m. Therefore, the following operating schedule, shown in Table 10, can be implemented.

Table 10: Summer operating schedule

Time period	Process	Comments
Sunshine (7AM-8PM)	Solar hydrogen production	- High solar intensity period in summer. - Suitable for solar hydrogen production.
Sunshine(7 AM-8PM)	Solar hydrogen energy storage	- High solar intensity period in summer with low energy demand. - Suitable for solar hydrogen production and storage
5PM-9PM	Solar hydrogen energy electricity generation	- Low solar intensity period in summer and high demand. - Suitable for electricity generation from stored hydrogen.

The yearly scenario can then be observed as shown in Figure 17. Summer scenario satisfies the fall and spring periods inclusive, where the solar intensity and the demand are approximately the same, according to Kib-tek [14].

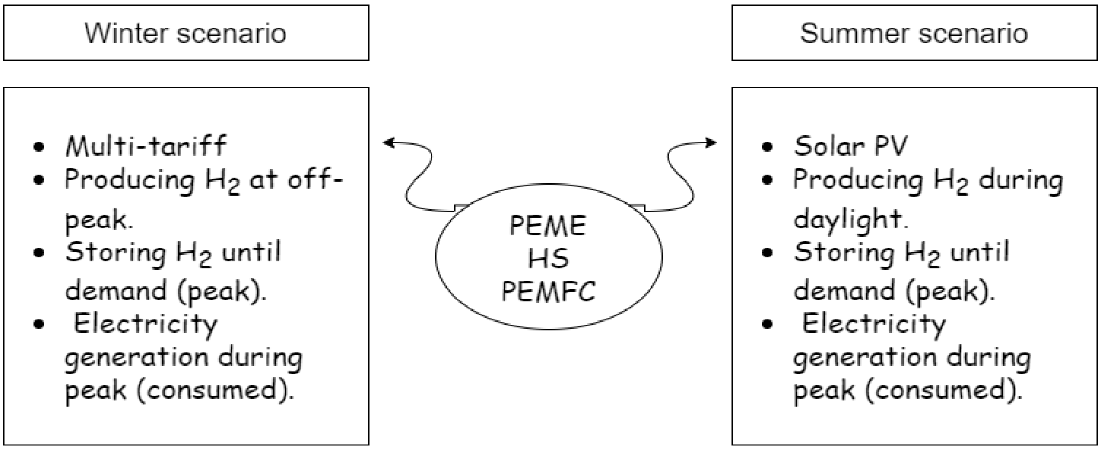

Figure 17: Yearly scenario

Chapter 4

METHODOLOGY

In this chapter, the sequence of methods followed to obtain favorable results are presented, as shown in Figure 18. In order to obtain economically feasible results, system optimization is essential. It can be understood from the literature review that PEM fuel cell efficiencies are low ranging between 40%-50% [49]. Therefore, thermodynamically optimizing the fuel cell efficiency is crucial. A PEMFC 1000kW is utilized in the current study, where the thermodynamically estimated and confirmed energy efficiency is 48.05%. The manufacturing company is Nedstack. In the thermodynamic analysis, the specifications of the Nedstack PEMFC 1000kW product is utilized.

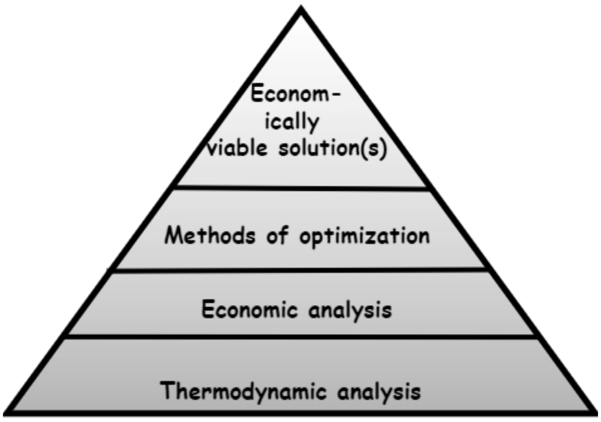

Figure 18: Methodology pyramid

After thermodynamic optimization of PEMFC 1000kW, the increased efficiency positively impacts the economic feasibility analysis, where less hydrogen would be utilized.

Finally, economic optimization is necessary through sensitivity analysis and Monte Carlo [77] simulation. The optimal results are selected to satisfy economic feasibility.

4.1 Thermodynamic analysis

The thermodynamic analysis of the most critical components includes the electrolyzer and fuel cell. The thermodynamics of the electrolyzer relates to its efficiency in order to obtain the amount of water inlet required to produce the necessary amount of hydrogen for the fuel cell. Consequently, the required amount of hydrogen inlet into the fuel cell depends on the fuel cell efficiency; as the efficiency increases, the required inlet hydrogen decreases.

4.1.1 Thermodynamic parameters of PEME

An electrolyzer can be denoted as a device that uses electrical power to produce hydrogen. PEM electrolyzers typically use 39.4 kWh to produce 1 kg of hydrogen [19]. Therefore, electrolyzer efficiency can be denoted as the energy content of the hydrogen produced divided by the input power, shown in Eq.(1). The energy content of hydrogen is its higher heating value, which is 142 MJ/kg (equivalent to 39.4 kWh/kg) [78,79]. According to reference [8], current electrolyzer efficiencies have reached 76%.

$$\eta_{ez} = \frac{LHV_{H_2} \times \dot{m}_{H_2}}{\dot{W}_{in}} \quad (1)$$

where, LHV_{H_2} Is the higher heating value of hydrogen, $\dot{m}_{H_2}$ Is the outlet mass flow rate of hydrogen produced, and $\dot{W}_{in}$ is the input power, assuming no heat is coming from an external heat source.

Furthermore, according to the reversible chemical reaction of $H_2O \rightleftarrows H_2 + \frac{1}{2}O_2$, the balance requires that the same amount of water inlet is the same amount of hydrogen outlet, and half of that quantity is oxygen. However, the electrolysis efficiency affects the effectivity of the reaction as it requires around 9L of H_2O to produce 1 kgH_2. Therefore, a polymer electrolyte membrane electrolyzer (PEME) can be described as a device, where water and electricity are provided as inlets to the control volume, and hydrogen and oxygen are outlets from the control volume. In consequence, a mass balance can be derived from Figure 19 as follows;

$$\dot{m}_{in} = \dot{m}_{out} \tag{2}$$

$$\dot{m}_{H_2O} = \dot{m}_{H_2} + \dot{m}_{O_2} \tag{3}$$

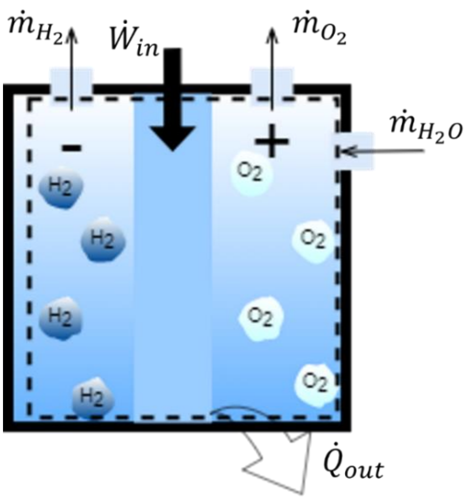

Figure 19: Electrolyzer mass and energy balance

4.1.2 Thermodynamic parameters of PEMFC (exergetic analysis)

Exergy is a property that determines the useful work potential of a given amount of energy at a specified state. It is also called the availability or available energy [46]. In an exergy analysis, the work output is maximized when the process is evaluated in a reversible manner between two specified states. The initial state is specified and not variable and the final state is in thermodynamic equilibrium with the surrounding and is called the dead state [46].

Exergy can be transferred through heat, work, and mass. It shows the exergy gained or lost by the system throughout the process [46]. The exergy or work potential of a flow can be expressed as follows;

$$\psi = (h - h_0) - T_0(s - s_0) + \frac{V^2}{2} + gz \tag{4}$$

where, h is the enthalpy at the initial state, T_0 is the dead state temperature, V is the velocity, and z is the height or distance. All subscript (0) denote the property at the dead state.

This exergy, ψ, indicates the maximum amount of useful work under reversible conditions as the system changes states, and represents the reversible work, W_{rev} [46].

The actual output work of a fuel cell stack is in terms of voltage, current, and number of cells in a stack, as shown below [48,66];

$$\dot{W} = IV_{cell}N_{cells} \tag{5}$$

$$V_{cell} = \frac{2.02 \times 10^{-3}\dot{W}_{elect}}{2F\dot{n}_{H_2}} \tag{6}$$

where, *F* is Faraday's constant equivalent to 96,485.34 A sec/mol.

The molar flow rate, $\dot{n}_{H_2}$, can be found using Eq. (7), where M_{H_2} is the molar mass of hydrogen, and then the number of cells can be found via Eq. (8).

$$\dot{n}_{H_2} = \frac{\dot{m}_{H_2}}{M_{H_2}} \tag{7}$$

$$N = \frac{2F\dot{n}_{H_2}}{I} \tag{8}$$

Furthermore, an energy balance can be derived where hydrogen and air are inlets to the control volume and water, heat, and electric power are outlets of the control volume, as illustrated in Figure 20.

Then, an energy balance equation can be derived, as shown below;

$$\dot{Q}_{H_2,in} + \dot{Q}_{air,in} = \dot{W}_{elec} + \dot{Q}_{H_2O} + \dot{Q}_{H_2,out} + \dot{Q}_{air,out} + \dot{Q}_{lost} \tag{9}$$

where, $\dot{Q}_{H_2,in}$ is the inlet energy carried by hydrogen, $\dot{Q}_{air,in}$ is the inlet energy carried by air, $\dot{W}_{elec}$ is the output power produced, $\dot{Q}_{H_2O}$ is the energy carried by water, $\dot{Q}_{H_2,out}$ is the energy carried by hydrogen at the end of the reaction, $\dot{Q}_{air,out}$ is the energy carried by air at the end of the reaction, and $\dot{Q}_{lost}$ is the energy lost due to the reaction.

Based on the energy balance derived from Eq.(9), the inlet and outlet energy carried by hydrogen can be expressed as the total hydrogen energy in the reaction and denoted as $\dot{Q}_{H_2}$. $\dot{Q}_{H_2}$ Is the difference between the inlet hydrogen energy $\dot{Q}_{H_2,in}$ And the outlet hydrogen energy $\dot{Q}_{H_2,out}$. Likewise, the inlet and outlet energy carried by air can be expressed as the total energy content of air during the reaction and can be denoted as $\dot{Q}_{air}$. $\dot{Q}_{air}$ Is the difference between the inlet energy in air $\dot{Q}_{air,in}$ And the outlet energy carried by air $\dot{Q}_{air,out}$.

Based on Eq.(4), the flow exergy is a function of enthalpy, entropy, kinetic energy, and potential energy. However, in the present thermodynamic analysis, the following assumptions are utilized:

- Steady flow,
- Steady state,
- And negligible kinetic and potential energy changes[80].

Moreover, a relation can be obtained between the reversible work and the actual produced work, or useful work, W_u. The difference between the maximum potential work (W_{rev}) and the useful work (W_u) is called exergy destroyed. The reason a device cannot produce its maximum work potential is due to irreversibilities. Irreversibilities are equivalent to exergy destroyed [46]. Irreversibilities generate entropy, and anything that generates entropy destroys exergy. Therefore, exergy destroyed is proportional to the entropy generated, as shown below and is always present in an irreversible system.

$$X_{dest} = T_0 S_{gen} \tag{10}$$

where, S_{gen} is the entropy generated.

Exergy balance determines the flow of exergy carrying substances into the system. Through the energy balance, exergy transfer through heat can be obtained. Reducing Eq.(9) to Eq.(11), the actual heat lost can be estimated through equating all inlet energy to all outlet energy.

$$\dot{Q}_{H_2,in} + \dot{Q}_{air,in} = \dot{W}_{elec} + \dot{Q}_{lost} + \dot{Q}_{H_2O,out} + \dot{Q}_{exhaust} \tag{11}$$

Then, exergy transfer by heat can be obtained using Eq.(12).

$$\dot{X}_{heat} = \left(1 - \frac{T_0}{T}\right) \dot{Q} \times r_{HL} \tag{12}$$

where, r_{HL} is the heat loss ratio in a fuel cell (equivalent to 20%) [67,68].

However, in a chemical reaction, the heat transfer due to the reactants and products is equal to the difference between the enthalpy of the products and the enthalpy of the reactants. Therefore, the energy balance relation in Eq.(13) of a steady-flow can be expanded as shown below;

$$\dot{E}_{in} = \dot{E}_{out} \quad (13)$$

$$\dot{Q}_{in} + \dot{W}_{in} + \dot{n}_r h_{react} = \dot{Q}_{out} + \dot{W}_{out} + \dot{n}_p h_{prod} \quad (14)$$

where, $\dot{n}_r$ is the molar flow rate of the reactants and h_{react} is the specific enthalpy of the reactants.

Moreover, the chemical energy of a reactant or a product is represented at a reference state. Enthalpy of formation, $\bar{h}_f$, is the property that can be identified as the enthalpy at a specified state due to the chemical composition of the substance. Also, when analyzing reacting systems, the property values must be relative to the standard reference state STP[2]. The standard reference state is denoted by a superscript (°). Therefore, the enthalpy of a reactant or product becomes;

$$H_{react} = N_r\left(\bar{h}_f + \bar{h} - \bar{h}^{\circ}\right)_{react} \quad (15)$$

where, $\bar{h}$ is the sensible[3] enthalpy at the specified state.

Hence, Eq.(14) can be further reduced to Eq.(16).

$$Q - W = H_{prod} - H_{react} \quad (16)$$

Furthermore, exergy transfer by mass is simply the mass flow with exergy content. It is the product of the mass by the exergy, as shown below;

$$\dot{X}_{mass} = \dot{m}\psi \quad (17)$$

Finally, exergy transfer by work is the useful work potential. Thus, it can be expressed as;

$$\dot{X}_{work} = \dot{W} \quad (18)$$

[2] STP stands for standard temperature and pressure of 25°C and 1atm, respectively.
[3] Change of enthalpy due to temperature, not accompanied by phase change.

In consequence, the exergy balance of the PEMFC can be obtained by equating all the exergy inlets to all the exergy outlets inside the control volume. Shown in Figure 20, the inlet exergy transfer is transported by masses of oxygen and hydrogen. However, the outlet exergy transfer is transported by work ($\dot{X}_w$), heat ($\dot{X}_Q$), mass of exhaust air, and mass of water vapor.

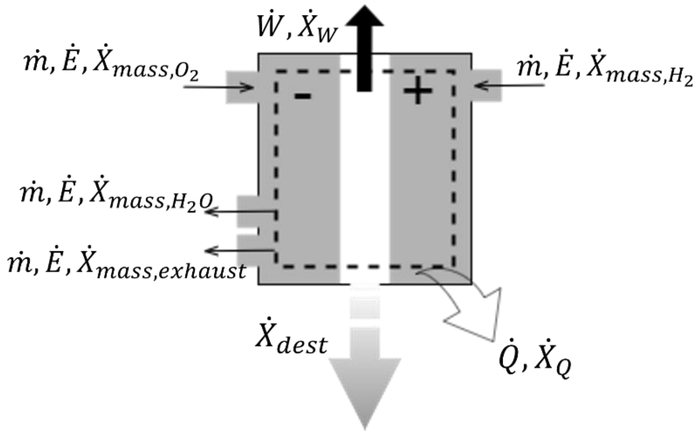

Figure 20: PEMFC mass, energy, and exergy balance

Hence, an exergy balance equation can be derived by equating all the exergy flow inlets to all the exergy flow outlets, as shown below [81];

$$\dot{X}_{H_2} + \dot{X}_{O_2} = \dot{X}_w + \dot{X}_Q + \dot{X}_{H_2O} + \dot{X}_{exhaust} + \dot{X}_{dest} \tag{19}$$

Finally, the exergy balance for a chemical reaction can be written as;

$$\dot{X}_2 - \dot{X}_1 = \dot{X}_Q + \dot{X}_w + \dot{X}_{dest} \tag{20}$$

where, $\dot{X}_1$& $\dot{X}_2$ is the exergy transfer through mass of the reactants and the products and can be obtained;

$$\dot{X}_{1,2} = \sum \dot{m}_i \psi_i \tag{21}$$

where, i represents the reactants and the products.

Exergy destroyed represents the lost work potential and is also called the irreversibility or lost work. Exergy destruction is a positive quantity for actual processes. Therefore, $T_0\dot{S}_{gen} \geq 0$. To decrease exergy destruction, irreversibilities of the system have to be reduced. The reduction of irreversibilities depends on what component and how much it contributes to exergy destruction. Knowing the most critical component(s) that impact the exergy destruction helps reduce the exergy destruction caused by this certain component.

Thus, exergy destruction can be identified as the difference between the maximum work potential of the system and the actual work produced, as shown below;

$$\dot{X}_{dest} = \dot{W}_{rev} - \dot{W}_u \tag{22}$$

In any work producing system, the reversible work, $\dot{W}_{rev}$, is always greater than the actual produced work, $\dot{W}_u$ [74].

4.1.2.1 Energetic and exergetic efficiencies

The first-law efficiency of steady-flow devices applies to the ratio of the converted net work output to total heat or energy supplied. In other words the first-law efficiency is the energetic efficiency. It is associated with the energy supplied to the system. Therefore, the first-law efficiency, η_I, of an electrochemical reaction can be denoted as the net work output to the energy supplied by the fuel.

$$\eta_I = \frac{\dot{W}_{out}}{LHV_{H_2} \times \dot{m}_{H_2}} \tag{23}$$

where *LHV* is the lower heating value which is used when the outlet water is in the vapor state [66].

Furthermore, the maximum energetic efficiency, $\eta_{I,max}$, of an electrochemical reaction can be obtained by using the reversible work, W_{rev}.

$$\eta_{I,max} = \frac{\dot{W}_{rev}}{LHV_{H_2} \times \dot{m}_{H_2}} \tag{24}$$

However, the first-law efficiency does not portray the best performance, and thus it is not a realistic measure.

The second-law efficiency of a steady state flow is a measure of how closely a system approximates to a reversible process. It resembles a range of available potential improvements [74]. The second-law efficiency is the exergetic efficiency. It can be determined as the ratio of the actual performance to the best possible performance under the same conditions. According to reference [46], the second law efficiency is equal to the ratio of the exergy recovered to the exergy supplied. Therefore, for an electrochemical reaction, the second-law efficiency, η_{II}, can be denoted as the ratio of the actual work output to the exergy supplied of the reactants, as shown in Eq.(25) [67].

$$\eta_{II} = \frac{\dot{W}_{out}}{\dot{X}_{H_2} + \dot{X}_{O_2}} \tag{25}$$

Moreover, the maximum exergetic efficiency, $\eta_{II,max}$, of an electrochemical reaction can be obtained by using the reversible work, W_{rev}.

$$\eta_{II,max} = \frac{\dot{W}_{rev}}{\dot{X}_{H_2} + \dot{X}_{O_2}} \tag{26}$$

The exergy of a chemical substance is divided into chemical (X_{ch}) and physical (X_{ph}) exergies. X_{ch} Is obtained through standard known chemical exergy tables [82]. X_{ph} For gases is obtained through Eq.(28).

$$\dot{X}_i = \dot{m}_i\left(X_{ch} + X_{ph}\right) \tag{27}$$

$$X_{ph} = c_p T_0 \left[\frac{T}{T_0} - 1 - ln\left(\frac{T}{T_0}\right) + ln\left(\frac{P}{P_0}\right)^{\frac{k-1}{k}} \right] \tag{28}$$

where, k is the ratio of specific heat at constant pressure to specific heat at constant volume (can be obtained from thermodynamics tables) [66].

Furthermore, c_p Can be obtained for specific temperatures using Eq.(29), where values *a*,*b*,*c*,*d* are constants and can be obtained from thermodynamics property tables (Table A-2 in Ref. [46]);

$$c_p = a + bT + cT^2 + dT^3 \tag{29}$$

4.1.2.2 PEMFC 1000kW Nedstack product specifications

According to the product manufacturer, a minimum 25% of the total hydrogen provided is excess hydrogen, which is recirculated to remove droplets at the cathode caused by outlet water [83]. The outlet water is heat carrying, pure, demineralized liquid water, called H_2O drain. The pure water is available for the humidification of hydrogen and air, nevertheless, it can be used for other purposes [83].

Figure 21: Nedstack PEMFC appearance impression [83]

In the present research, PemGen 1000 fuel cell stack from Nedstack, shown in Figure 21, [83] is utilized. Four units of the 1000 kWe fuel cell stack is economically and technically investigated to match the power demand of 15 MWh. The implemented membrane material is Per Fluor Sulfonic Acid [83]. In a stack, PEM fuel cells (PEMFC) are connected in series at a usable voltage [83]. According to the manufacturers, the current PEMFC efficiency is 48.05% [83]. The operating conditions, provided in Figure 22 of the 1000 kWe PEMFC include hydrogen and air operating temperature and pressure of 65℃ and 6 barg[4], respectively. Also, as seen in Figure 22, the inlet mass flow rates of hydrogen and air are 85 kg/h and 4686 kg/h, respectively. According to Nedtsack, the produced water due to the reaction tends to form droplets that obstruct the flow of oxygen through the cathode. Thus, the flow of air is required to contain twice as much oxygen as the consumed quantity [83]. The system diagram is shown in Figure 23

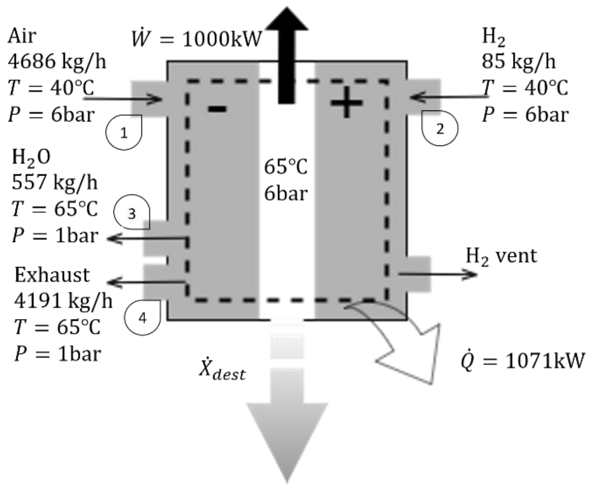

Figure 22: Nedstack PEMFC1000kW stack specifications [83]

4.2 Economic feasibility analysis

Following the selection of system components, an economic feasibility analysis is essential to determine the real potential returns of the investment [84]. An economic feasibility analysis will provide results in terms of net present value of profits (NPV).

[4] barg is a unit of gauge pressure with reference to atmospheric pressure at 1 atm.

This allows a straightforward way to make investment decisions. For example, if an NPV of an economic feasibility study is below zero, the investment is considered non-profitable [27]. Economic feasibility analysis results can also be demonstrated in terms of savings-to-investment ratio (SIR) [85]. SIR tells the investors and stakeholders whether the project will have a positive cash flow [85]. In a case of positive cash flow, the savings-to-investment ratio will be greater than 1 [86]. Therefore, it can be understood that economic feasibility analysis depends on investment costs, net profit, and savings.

$$SIR = \frac{C_{savings}}{C_{investment}} \tag{30}$$

$$NPV = C_{savings} - C_{investment} \tag{31}$$

Table 11: Economic feasibility input variables

Initial investment	**Cost**	**Annual investment**	**Cost**	**Lifetime**	**References**
PEME	6($/kg$H_2$)	O&M	3.96($/kg$H_2$)	25000 hours	[26]
H2 storage tank	650($/kg$H_2$)	O&M	-	20 years	[73]
PEMFC	1530000($)	O&M	5%CC($)	25000 hours	[83]

In the present research, the economic feasibility of integrating winter and summer scenarios hydrogen storage throughout the year is investigated. Initial investment costs include cost of the electrolyzer stack, cost of the hydrogen storage tank, and cost of the fuel cell stack. Based on the lifetime, shown in Table 11, collected from reference [26] in hours, the approximated lifetime in years can be obtained by knowing the working schedule of the PEME. Similarly, based on reference [83] provided by Nedstack, a working schedule for the PEMFC can be engineered to obtain the yearly lifetime of the fuel cell stack. Furthermore, annual investments include the annual operation and maintenance (O&M) for PEME and PEMFC. The annual O&M for PEMFC is 5 percent of its capital cost (CC)[83].

Moreover, the "reference" system to the "challenging" combined winter and summer scenarios is the thermal power plant generated electricity. Hence, the thermal power plant electricity prices in North Cyprus are used in the present economic feasibility study under multi-tariff electricity billing. The electricity prices in North Cyprus currently follow a constant rate system, effective July, 2022, where each kWh range has a specific price, as shown in Table 12 [23].

Moreover, the electricity prices are expected to further increase, according to Kib-tek [23]. The night tariff (peak) used to be 0.092 USD/kWh in 2021 [14]. This means that the tariff has increased by 0.1 USD in less than one year, which is equivalent to 1.727 TL. The exchange rate used is 17.27 TL/USD.

Table 12: N.Cyprus electricity prices during summer effective July, 2022 [23]

Tariff name in kWh	**Price (TL/kWh)**	**Price ($/kWh)**
Night tariff	4.62	0.27
0-250	1.61	0.09
251-500	3.32	0.19
501-750	3.57	0.21
751-1000	3.84	0.22
1001 and above	4.62	0.27
Tourism sector	3.23	0.2

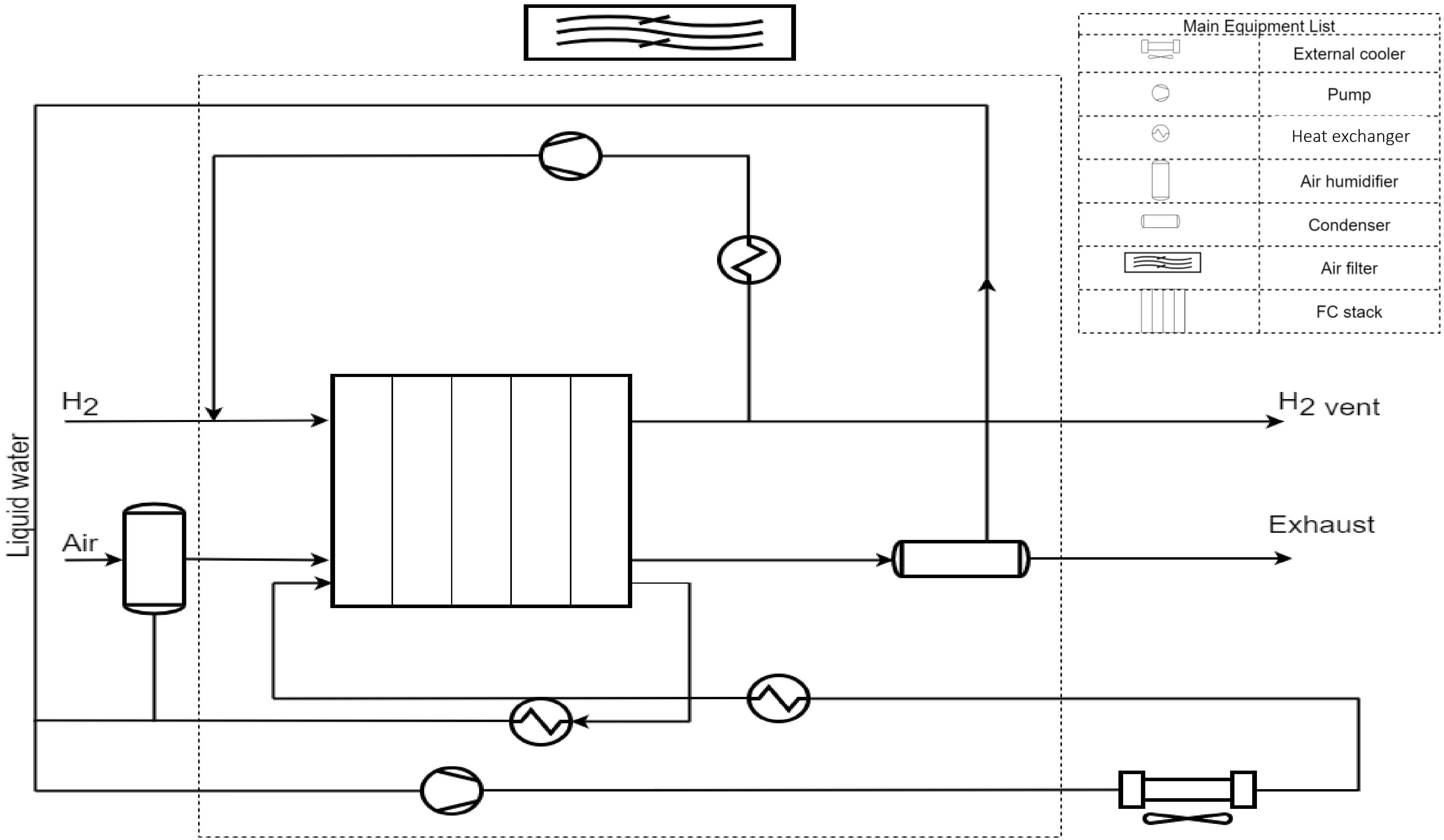

Figure 23: FC system diagram

4.2.1 Waste management in economic analysis

Development of cost management strategies depends on the local regulations and the value of waste cost compared with other production factors [47]. According to Giovanni [47], waste management is performed in three main ways: (1) waste reduction via clean technologies, (2) waste elimination, and (3) recycling waste to be used as raw material or energy. Figure 24 shows the proposed system with energy strategy and waste management. The wasted outlets of the system include;

- Heat carrying water vapor and excess hydrogen from the PEMFC,
- And oxygen from the PEME.

According to Nedstack, the excess hydrogen leaving the PEMFC is recirculated into the fuel cell [83]. However, the heated water vapor can be put to other uses. For example, the energy content in the water vapor in form of heat can be partially recovered by means of heat exchangers to be used in the process or for space heating [47,83].

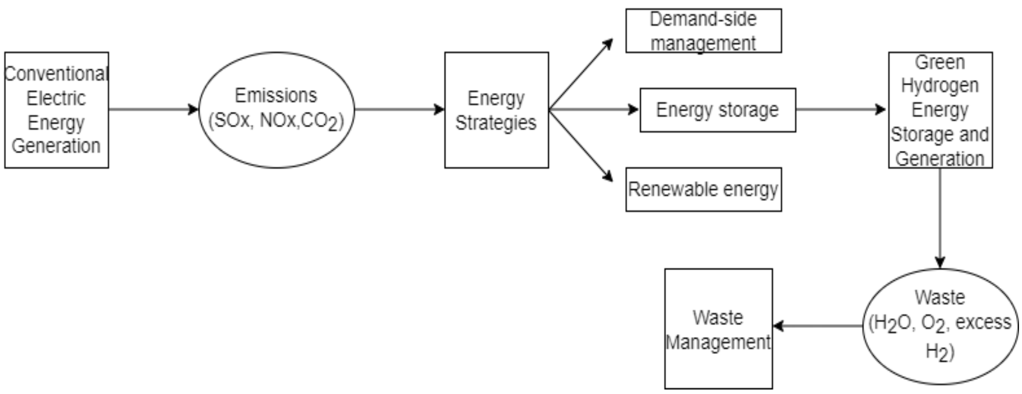

Figure 24: Energy strategy and waste management

Furthermore, the oxygen produced by the PEME is pure oxygen [36], which allows it to be stored and sold for profit instead of being wasted. According to a review made by Takeyoshi et al. [87], medical oxygen demand makes 1.1% of the total oxygen demand. The selling prices of oxygen are very high ranging from 0.6UScent/kgO_2 to 24.5US$/kg$O_2$ [87]. In the present economic feasibility study, an average will be taken, which is equivalent to 12.55US$/kg$O_2$. Moreover, excess generated electricity by the PEMFC can be sold to the power plant at the electricity tariff price, as illustrated in Figure 25.

4.2.2 Mathematical parameters

The present economic analysis is a comparison between the proposed system, hydrogen storage, and thermal power plant electricity generation. Therefore, the reference system is the grid connection challenged by hydrogen storage. The results of the current economic analysis will determine the investment decision.

4.2.2.1 Reference system

The thermal power plant will comprise of no new investment costs. However, electricity prices will be used. The aim of the present research is to fulfill a capacity of 15MWh during summer and winter for a hotels region. Hence, the electricity cost will be consumed electricity multiplied by the electricity tariff price, as shown below;

$$C_e = P \times c_e \tag{32}$$

where, P is the daily consumed electricity, and c_e is the tariff electricity cost.

To find the cost of electricity paid by summer, the daily power consumed is multiplied by the number of summer days per year. Then, the present value for each year can be obtained using;

$$C_{e,s} = \frac{P \times c_e \times 275}{(1+r)^t} \tag{33}$$

where, $C_{e,s}$ is the present value of electricity paid per summer, r is the discount rate, and t is the number of years.

The same equation can be used for winter calculation, where the number of days is 90.

4.2.2.2 Challenging system

The total investment cost, C_{tot}, is the sum of all capital costs including electrolyzer unit cost c_{ez}, fuel cell stack cost C_{FC}, and hydrogen storage tank unit cost, c_{st}.

$$C_{tot} = C_{ez} + C_{FC} + C_{st} \tag{34}$$

The lifetime in years of the electrolyzer stack and fuel stack can be obtained as follows;

$$L_y = \frac{t_{L,hr}}{t_{opt,hr} \times 365} \tag{35}$$

where, $t_{L,hr}$ is the lifetime in hours, and $t_{opt,hr}$ is the operation duration in hours.

Moreover, the unit costs of the electrolyzer and the storage tank are in \$/kgh$_2$. Therefore, the mass of hydrogen required to satisfy the capacity of the hotels region is critical in the present economic analysis. Eq.(23) is used to estimate the mass of hydrogen required to fulfill the 15MWh capacity. Subsequently, the capital costs of the electrolyzer and the hydrogen storage tank can be obtained,

$$C_i = m_{H_2} \times c_i \tag{36}$$

where, m_{H_2}Is the mass of hydrogen, and c_i is the unit cost of component *i*.

However, due to the efficiencies of the electrolyzer stack and the fuel stack, actual hydrogen mass calculations are required. Using Eq.(37), the useful hydrogen mass produced from the electrolyzer stack can be obtained. Since the storage tank efficiency is 95%, the produced hydrogen loses some of its mass [73].

$$m_{H_2} = \frac{m_{H_2,req}}{\eta_{st}} \tag{37}$$

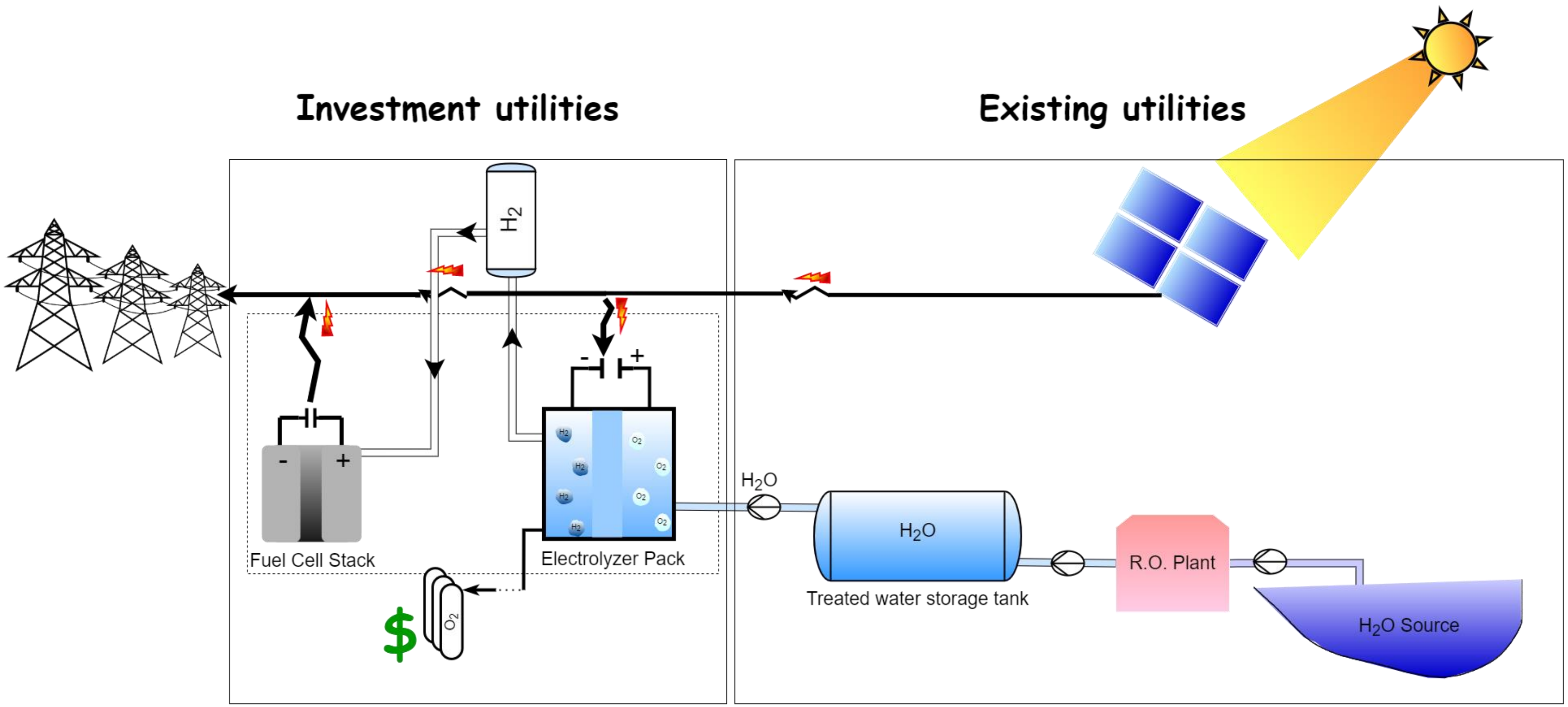

Figure 25: Hydrogen energy storage and electricity generation with waste management

where, $m_{H_2,req}$ is the required mass of hydrogen without losing some of its mass due to the hydrogen storage tank efficiency η_{st}.

Figure 26 shows the comparison between the total costs of the “reference” system and the “challenging” system. It can be seen that there is no initial investment for the existing thermal power plant grid connection. However, electricity price is vital to the current economic analysis. On the other hand, new investment cost to purchase the operating equipment (electrolyzer stack, hydrogen storage tank, and fuel cell stacks) is approximately $11.1 million and the re-investment cost of electrolyzer membrane after 25000 hours of operation is approximately $151,270. The efficiencies of each component can be seen, where the electrolyzer efficiency has been neglected in the present economic analysis as it does not vastly affect the economical parameters. Also, the storage tank efficiency is considerably high compared to the electrolyzer and fuel cell efficiencies. Hence, any improvements to enhance the hydrogen storage tank efficiency will be trivial.

Table 11 shows that O&M is paid for the electrolyzer stack and fuel cell stack. According to Nedstack, O&M is 5% of the capital cost (CC) [83]. Also, based on the estimations done by Boreum et al.[26], the O&M cost makes approximately 66% of the total unit cost. Consequently, the present value of the annual O&M can be obtained using the following equation;

$$C_{O\&M_s} = \frac{\sum C_{O\&M_i}}{(1+r)^t} \tag{38}$$

where, $\sum C_{O\&M_i}$Is the cost of O&M for component i.

Therefore, the total savings and the present value of the total savings can be obtained via Eq.(39) & (40), respectively.

$$C_{savings} = \sum C_{x,R} - \sum C_{x,C} \tag{39}$$

where, $C_{x,R}$ is the cost of annual expenditures (x) of the reference system, and $C_{x,C}$ is the cost of the annual expenditures (x) of the challenging system.

$$C_{savings,s} = \frac{C_{savings}}{(1+r)^t} \tag{40}$$

4.3 Methods of optimization

In this sections, methods to optimize the economic feasibility of the winter and summer scenarios are addressed. In order to optimize, a sensitivity analysis has to be carried out to identify the most critical input variables on the results. Following the sensitivity analysis, a scenario analysis is completed. In a scenario analysis, results are observed under different input variables that are selected through the sensitivity analysis. Monte Carlo is a software that generates thousands of scenarios under given constraints and distributions.

4.3.1 Sensitivity analysis

It can be seen from Figure 26 that the fuel cell efficiency is the lowest compared to that of the electrolyzer and the storage tank efficiencies. Also, according to Kib-tek [14], the electricity tariff prices are expected to further increase, meaning that the results obtained in the current work are on the conservative side. Also, according to U.S. Department of Energy, the hydrogen storage tank prices are expected to further decrease by the year 2025 [88]. Additionally, the unit cost of hydrogen production is expected to decrease to a market price of 5.74\$/kgh$_2$, according to U.S. Department of Energy [34]. Hence, a sensitivity analysis is critical to determine the most effective or impactful input variables on the SIR of the project.

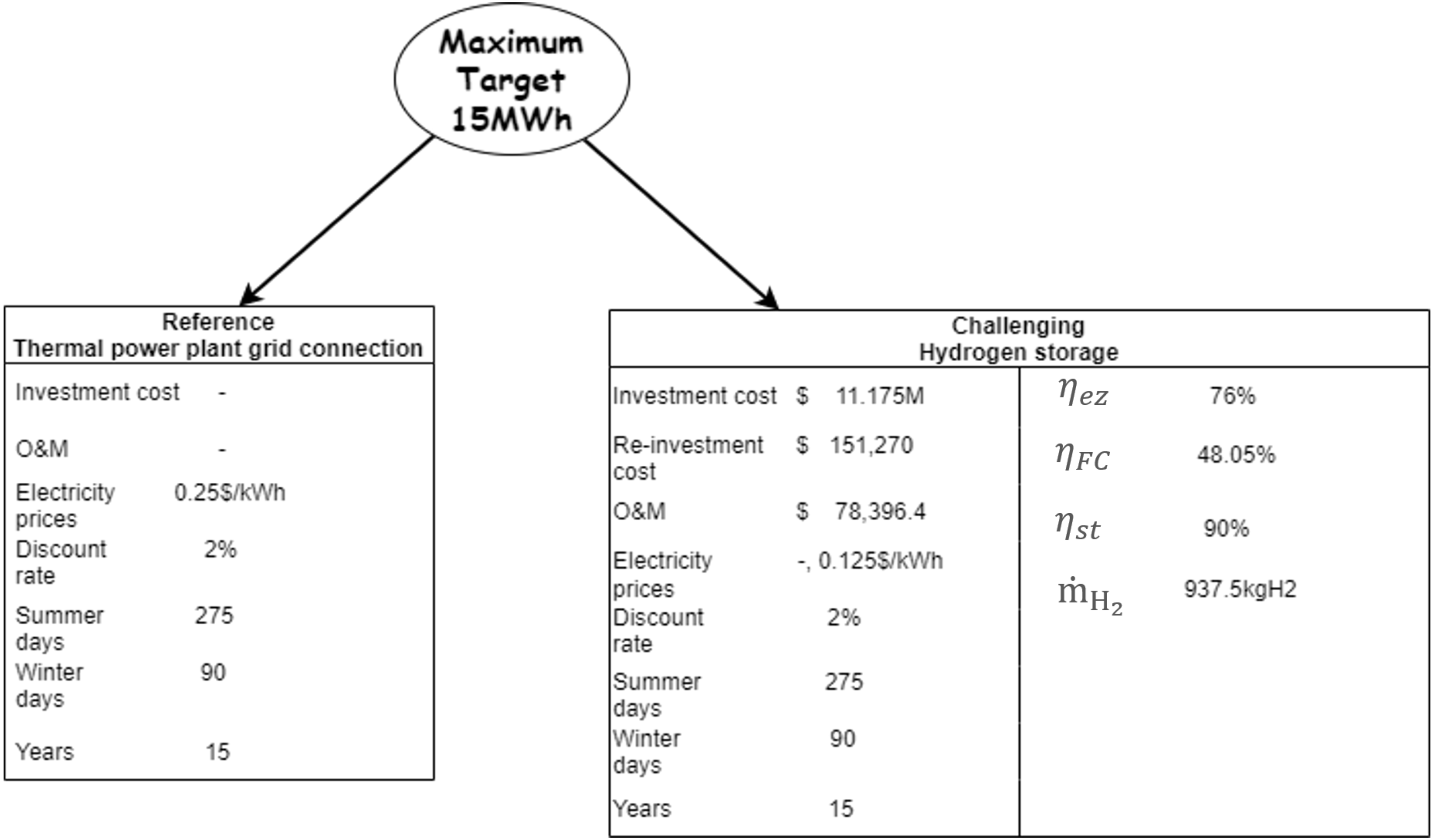

Figure 26: Reference and challenging systems' billing diagram comparison

The sensitivity analysis can be carried out by changing one variable and keeping the other variables constant and observing the effect on the project outcome.

$$SIR(a, b, c, f, g, h, x, y, z) \tag{41}$$

where, a is the daily power consumed, b is the daily operation hours, c is the fuel cell efficiency, f is the unit cost of the electrolyzer, g is the unit cost of the storage tank(s), h is the unit cost of the fuel cell, x is the electricity tariff price, y is the unit cost of O&M of the electrolyzer, and z is the unit cost of the O&M of the fuel cell.

4.3.2 Monte Carlo simulation

Optimizing results for the thermodynamics of the fuel cell optimizes the economic feasibility of the year round winter and summer scenarios. In order to carry out a Monte Carlo simulation, input and output variables, correlations, and probability distributions are parameters that need to be set. For the present study, the parameters are set according to Figure 27.

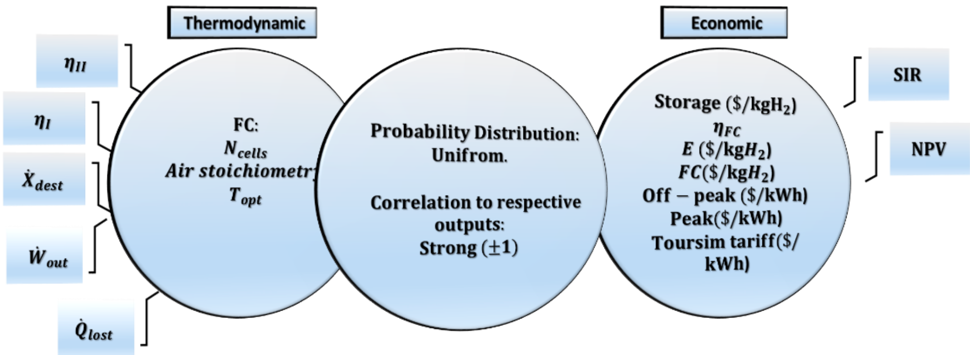

Figure 27: Monte Carlo set-up

The relations, or equations, that bind a respective input to an or a set of output(s) are added to the excel sheet, where the Mote Carlo software is integrated.

The thermodynamic optimal scenario(s) for the fuel cell exergetic efficiency and exergy destruction is obtained through the most critical input variables decided by the sensitivity analysis. Following, an economic optimal scenario(s) is obtained for the complete system. Therefore, the highest obtainable efficiency from the fuel cell thermodynamic scenario simulation is utilized in the economic scenario simulation.

Chapter 5

RESULTS AND DISCUSSION

Based on the data collected from Nedstack on their product PEMFC 1000, the base case thermodynamic analysis could be computed. Then, Monte Carlo simulation is carried out to find the optimal energy efficiency, due to its current low efficiency, and least exergy destruction of the fuel cell. Consequently, the best case scenario is used in the economic feasibility analysis. Finally, the best case scenario of the economic feasibility (the feasible scenario) can be utilized.

5.1 Thermodynamic results and Monte Carlo simulation

The base case model with current of 2400A and voltage of 420V is shown in Table 13. It can be seen that the energetic efficiency is slightly higher than the exergetic efficiency, similar to the work done by [66], due to the fact the fuels have slightly higher exergy than energy [89]. It can also be seen that further thermodynamic improvement can be done to decrease the lost heat and exergy destruction

Table 13: Thermodynamic base case scenario (based on the PEMFC1000 system specifications)

	η_I%	η_{II}%	$\dot{W}$ (kW)	$\dot{X}_{dest}$ (kW)	$\dot{Q}_{lost}$ (kW)
Base case	48.05	45.94	1000	981.78	1071.21

Based on the sensitivity analysis results, there is strong positive correlations between the number of FC's in a stack and operating temperature; and system efficiencies and rate of work output. However, the air stoichiometry (λ) shares a strong positive correlation with only the exergetic efficiency. Air stoichiometry is the minimum amount of air required to complete the chemical reaction [74]. The air stoichiometry also has a weaker negative correlation with $\dot{X}_{dest}$ and $\dot{Q}_{lost}$ compared to N_{cells} and T_{opt} which have strong negative correlations.

Table 14: Thermodynamic sensitivity data

Sensitivity Data (Correlation)					
Assumptions	$\boldsymbol{\eta_I}$%	$\boldsymbol{\eta_{II}}$%	$\dot{\boldsymbol{W}}$ **(kW)**	$\dot{\boldsymbol{X}}_{\boldsymbol{dest}}$ **(kW)**	$\dot{\boldsymbol{Q}}_{\boldsymbol{lost}}$ **(kW)**
$\boldsymbol{\lambda}$	--	1.00	--	-0.7	-0.7
$\boldsymbol{N_{cells}}$	1.00	1.00	1.00	-1.00	-1.00
$\boldsymbol{T_{opt}}$	0.10	1.00	1.00	-1.00	-1.00

Monte Carlo simulation shows that the exergy efficiency increases with increasing air stoichiometry, operating temperature, and number of cells. That is due to an increase in the gross output power and decrease in heat losses.

Furthermore, it can be seen from Figure 29 that exergy destruction decreases with increasing T_{opt} due to the increase in η_{II}. It can be understood from the results the exergetic efficiency is inversely proportional to exergy destruction. Thus, it can be concluded that higher exergetic efficiencies represent low exergetic destruction. Higher operating temperature increases the enthalpy of the gases and the enthalpy drop in the PEMFC, which increases the work output at fixed mass flow rates [90]. Additionally, the increase in work output with respect to the number of cells agrees with research results from reference [67], as more cells allow for more fuel intake at constant current. The increase in exergetic efficiency with respect to the operating temperature agrees with research results by references [66] and [66]. It is also recommended by reference [66] that the air stoichiometry remains below 4. Increasing the air stoichiometry increases the amount of reacting O_2 with H_2, which reduces the amount of un-reacting hydrogen, reducing mass flow irreversibilities.

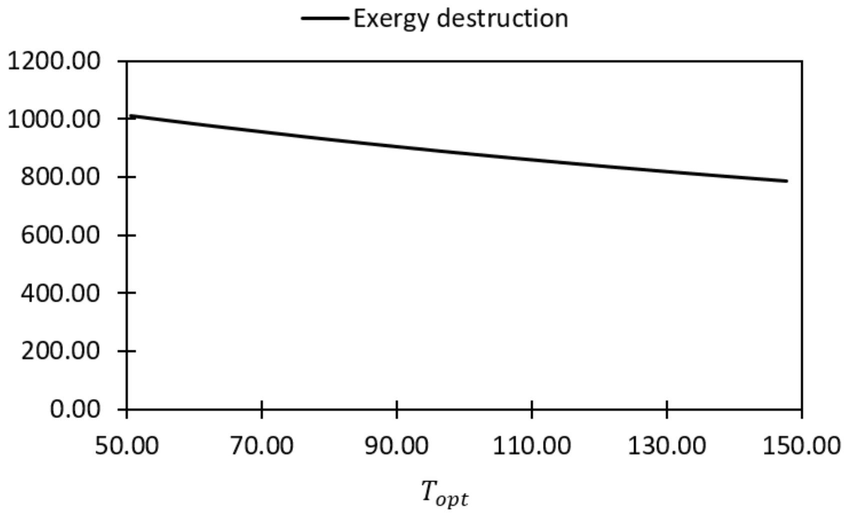

Figure 28: Variation of $\dot{X}_{dest}$ with T_{opt}

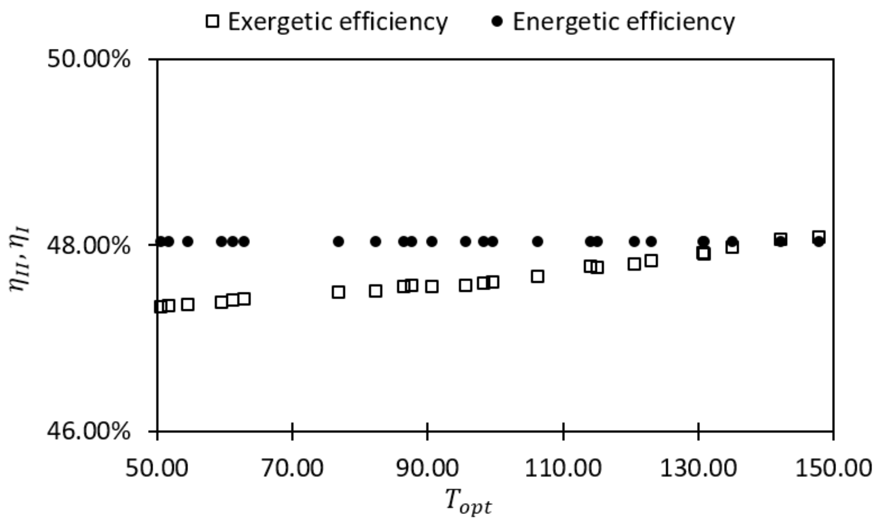

Figure 29: Variations of η_I, η_{II} with T_{opt}

It is clear from the results shown in Figure 31 that the maximum achievable exergetic and energetic efficiencies of the PEMFC1000 can reach 48.09% and 50.19%, respectively. Also, obtained from the sensitivity analysis data in Table 14,

$\lambda, T_{opt}, N_{cells}$ are the major factors that impact the exergy destruction, thus by manipulating their values, exergy destruction can be further reduced.

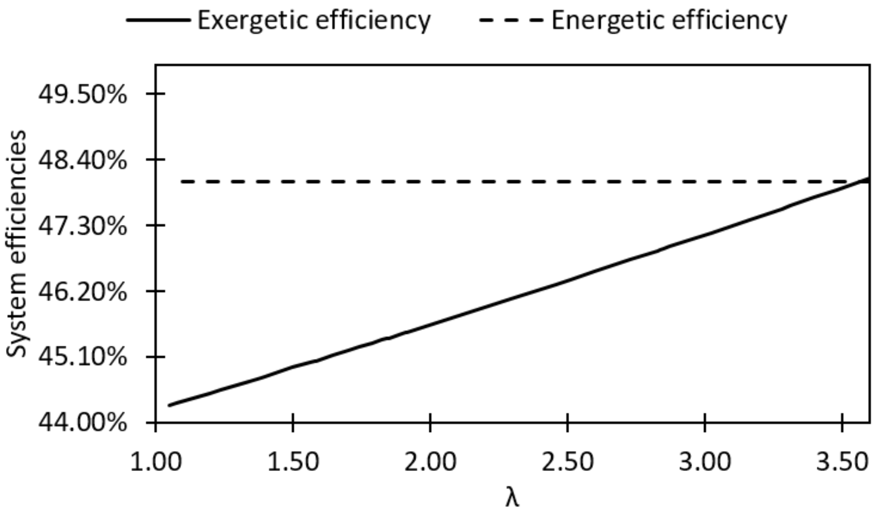

Figure 30: Variations of η_I, η_{II} with λ

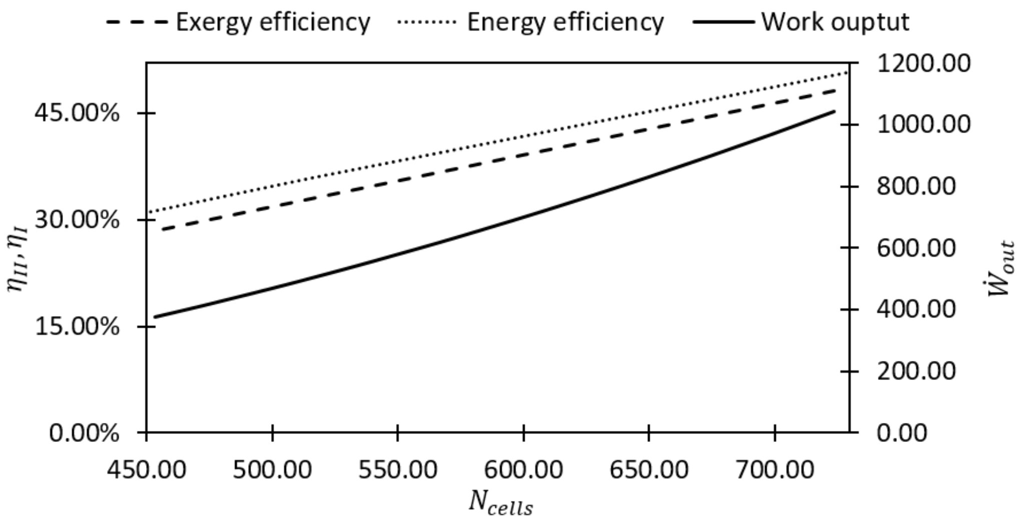

Figure 31: Variations $\eta_I, \eta_{II}, \dot{W}_{out}$ of with N_{cells}

Exergetic analysis has been carried out due to that fact that it examines the maximum potential of the reacting elements. Exergetic analysis measures the chemical and physical exergies of all reactants and products, it also helps understand how much potential a substance holds and how much the chemical and physical potential can be improved. Unlike energetic, or first law, analysis, exergetic analysis measures the irreversibilities of the system and allows for methods to reduce the irreversibilities caused by operating parameters and/or reacting elements. Energetic analysis, on the other hand, only examines the potential of the system through the energy content of the fuel (HHV or LHV) and a few operating parameters like N_{cells}. It disregards the physical and chemical potential of the other elements, as shown in Figure 28 and Figure 30 the energetic efficiency remains constant with changes in T_{opt} And λ.

Consequently from the results obtained, best, or optimal, and worst case scenarios can be extracted from the Monte Carlo simulation. The best case, shown in Table 15, with energetic efficiency of 50.19% is utilized in the economic feasibility analysis.

Table 15: Thermodynamic best, worst, and base case scenarios

	η_I%	η_{II}%	$\dot{W}$ (kW)	$\dot{X}_{dest}$ (kW)	$\dot{Q}_{lost}$ (kW)
Base case	48.05	45.94	1000	981.78	1071.21
Best case	50.19	48.09	1043.94	928.74	1025.68

5.2 Economic feasibility results and Monte Carlo simulation

The economic feasibility results based on equations demonstrated in section 4.2.2 show that the system is not feasible. The base case scenario in

Table 17 has a negative NPV, which means that the project is losing money rather than profiting.

The sensitivity data collected in Table 16 is largely satisfied as obtained by reference [18], where there is a strong correlation between the electricity prices, the fuel cell efficiency, and the NPV and SIR. However, the correlation between the unit costs of fuel cell and NPV and SIR is negative. Furthermore, the storage unit cost and electrolyzer efficiency and electrolyzer unit cost have weak correlations.

Table 16: Economic sensitivity data

Sensitivity Data (Correlations)		
Assumptions	**NPV**	**SIR**
$\eta_{ez}\%$	0.23	0.23
$\eta_{FC}\%$	0.95	0.95
Off-peak tariff($/**kWh**)	1.00	1.00
Peak tariff ($/**kWh**)	1.00	1.00
FC ($/**kg** H_2)	-0.35	-0.35
Ez ($/**kg** H_2)	-0.05	-0.05
St ($/**kg** H_2)	-0.03	-0.03

Table 17: Economic base case scenario

Base case	
$\eta_{FC}\%$	48.05
$\eta_{ez}\%$	76.00
Off-peak tariff($/**kWh**)	0.125
Peak tariff ($/**kWh**)	0.25
Ez ($/**kg** H_2)	6
FC ($/**kg** H_2)	2667
St ($/**kg** H_2)	650
SIR	0.4
NPV	-6.9E6

Furthermore, the economic feasibility analysis is applied on the winter and summer scenarios combined. The system breaks even at the scenario provided in Table 18. The break-even scenario denotes no losses or profits, thus SIR is 1 and NPV is 0.

It is observed from Table 18 that the fuel cell efficiency needs to increase by approximately 3.9% to reach a break-even point. Similarly, the storage and fuel cell unit cost needs to be reduced by at least 88.7% and 60.6% for feasibility, respectively. On the other hand, minor changes in the electrolyzer unit cost are required at break-even point and no change is required for electrolyzer efficiency due to its weak correlation.

Table 18: Economic base, best, and break-even scenarios

	Base case	**Best case**	**Break-even case**
η_{FC}%	48.05	50.19	50
η_{ez}%	76.00	76.00	76.00
Off-peak tariff ($/kWh)	0.125	1	0.2
Peak tariff ($/kWh)	0.25	2	0.4
Ez ($/kg H_2)	6.00	5.74	5.86
FC ($/kg H_2)	2667.00	1500	1770
St ($/kg H_2)	650.00	500	576.5
SIR	0.38	3.97	1.00
NPV	-7.25E+07	6.26E+07	0

It can also be seen that in all the cases the fuel cell efficiency has higher priority than the electrolyzer efficiency. This can be explained by the stronger correlation of the η_{FC} on the SIR.

While the obtained best case scenario seems implausible due to the expensive peak tariff, more plausible scenarios can be obtained to approximate the project to reality as much as possible. Figure 32 demonstrates the possible increase in SIR using best case scenario variables and changing only the tariff prices. The change in tariff in Figure 32 is more probable compared to the values in the best case scenario. It can be seen from Figure 32 that with 0.8 $/kWh peak tariff prices and 0.4 $/kWh off-peak price, the project is feasible with the best case scenario variables. Also, the SIR can reach 2 with peak tariff of 1.2 $/kWh.

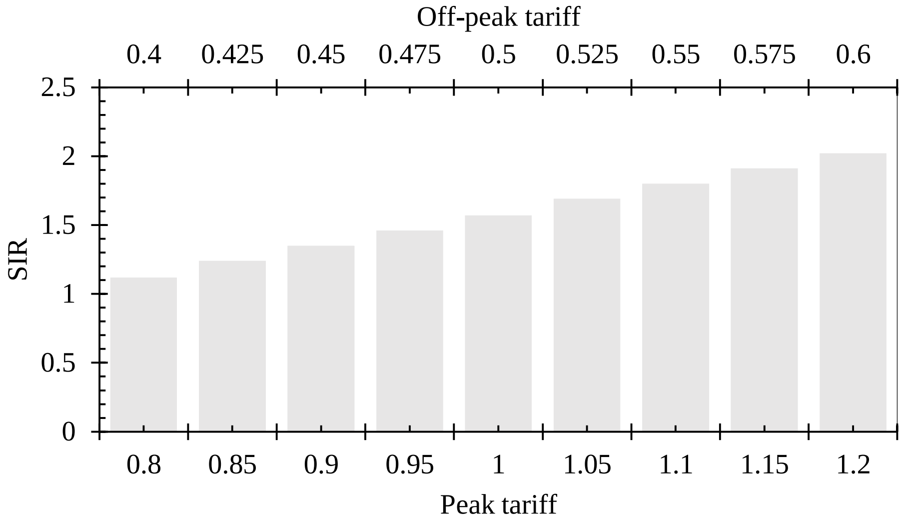

Figure 32: SIR with increasing peak tariff (off-peak tariff is half the peak tariff)

The economic feasibility results show potential economic viability. Similar to the study made by Boreum et al. [26] the sensitivity analysis data show that the electricity is the most impactful economic factor that affects the hydrogen production cost followed by the equipment unit costs. Moreover, the study made by reference [16]over a lifetime of 15 years and a discount rate of 2% show that the lowest electricity cost should be between 0.28 to 0.45 \$/kWh, where the capital cost is minimized up to 25%. Furthermore, according to reference [91], based on the sensitivity data the fuel cell efficiency shows significant impact on the economic feasibility, similar to the current study. Also, according to Curtiss [91], the competitive price of hydrogen production has to be decreased to 50\$/MWh with cost of electricity set to \$0 and the capital cost of fuel cell to be cut in half. Similar to the present study, the cost of electricity was set to \$0 assuming the utilization of an already existing solar energy electric cooperative, and the fuel cell unit cost had to be reduced to 1770 \$/kgH_2 from its current cost of 2667 \$/kgH_2.

Chapter 6

CONCLUSION

As a conclusion, the system scenario is currently non-feasible. However, with the scientific and technological advancements, unit costs of major system components can be reduced, as well as poor efficiencies can be enhanced. In addition, with the depletion of fossil fuels, their costs are rapidly increasing throughout the world, giving an advantage to hydrogen storage. The current investment costs are considerably high compared to the reference technology of electricity production through conventional power plants.

Furthermore, exergy analysis was necessary to obtain the true potential of the system. Energetic analysis was not enough to examine all the operating parameters and the fuel chemical and physical potentials.

Moreover, heat can be recovered from the outlet exhaust (saturated and depleted air), which is at 60℃ by integrating a heat exchanger. The heat could be used for water heating, space heating, or other purposes that would either save costs or create profit.

The present study offers a hydrogen storage system that can provide solutions including:

- Flattening the duck curve;

- Reducing thermal power plant and grid overloading by valley filling and peak shaving (peak shifting);
- Preserving fossil fuels;
- Reducing toxic gaseous emissions into the atmosphere.

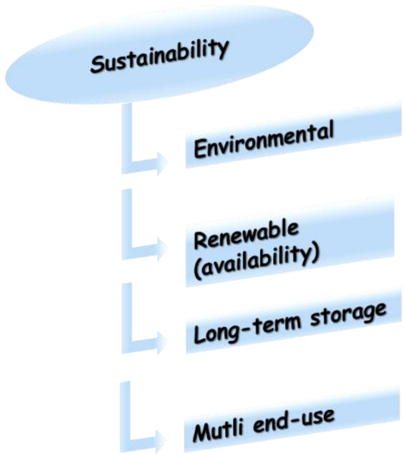

Figure 33: Hydrogen energy storage solution

Additionally, the system does not only have an economic potential, but it is also sustainable. This is because hydrogen maintains long periods of storage due to its high energy density, it is a renewable and abundant source which ensures its availability, and green hydrogen production using renewable energy sources is an environmental solution to energy storage and electricity generation. Hydrogen provides a multi end-use solution, where it can be converted to electrical energy, oxygen produced during electrolysis can be used for profit, and heat carrying, deionized water from the fuel cell can be utilized for heating purposes or the water can be recirculated back to the R.O. plant. Furthermore, the system has proven to be feasible as expected price reduction in fuel cell, electrolyzer, and storage unit costs by U.S. Department of Energy [38]. It can also be feasible as future electricity prices are expected to increase, according to Kib-tek [14]. Additionally, at off-peak and peak tariff ratios less than 0.5, the system approaches economic feasibility at lower peak tariff rates. For example, it has been observed that the system breaks even at peak tariff price of 0.35 $/kWh with an off-peak tariff price of 0.14$/kWh, which is a ratio of 0.4.

Furthermore, other methods of energy storage such as lithium ion batteries, which have an estimated life time of 10 years and disposal cost at the end of life in countries like Australia and the United States can be used as alternative due to their higher efficiencies, approximately 90%, according to Tesla [92]. However, the environmental cost, the short life time, the rapid deterioration, and rapid heat-up pose great threats on the environment and consumers. When stored for too long, the battery can degrade prematurely causing it not to reach its normal voltage range, posing the risk of being overcharged. This causes the release of chemical toxins during operation, which can be harmful to the environment and inhabitants [93]. Therefore, more environmentally friendly and longer life hydrogen storage is the future, where efficiency and cost improvements will allow for its viability.

Moreover, given the rising situation in Eastern Europe which was heavily reliant on Russian supplied gas for heating in winter and wind and solar energy for electricity in summer is threatened by instability in power supply, according to Euronews [94]. Also, the heat wave is affecting power plant production in Germany causing a reduction in electricity generation, inducing power cuts, due to the cooling water being slightly high in temperature [95]. This has created an increase in electricity prices which have surpassed 394 $/MWh in August, 2022 and created refuge to coal as energy source for heating during winter [96]. Coal emits more greenhouse emissions than any other energy source, causing deadly air pollution [97]. Additionally, according to Clean Energy Wire [97], home battery storage systems usually last only a few hours while the grid needs storage that would last for weeks. Therefore, hydrogen energy storage can be an effective solution for: the avoidance of power cuts, avoidance of coal utilization, and the required long periods of storage.

REFERENCES

[1] Ruhani B, Abidi A, Hussein AK, Younis O, Degani M, Sharifpur M. Numerical simulation of the effect of battery distance and inlet and outlet length on the cooling of cylindrical lithium-ion batteries and overall performance of thermal management system. J Energy Storage 2022;45. https://doi.org/10.1016/J.EST.2021.103714.

[2] Salehi M, Heidari P, Ruhani B, Kheradmand A, Purcar V, Căprărescu S. Theoretical and experimental analysis of surface roughness and adhesion forces of MEMS surfaces using a novel method for making a compound sputtering target. Coatings 2021;11. https://doi.org/10.3390/coatings11121551.

[3] Rivarolo M, Rattazzi D, Lamberti T, Magistri L. Clean energy production by PEM fuel cells on tourist ships: A time-dependent analysis. Int J Hydrogen Energy 2020;45:25747–57. https://doi.org/10.1016/J.IJHYDENE.2019.12.086.

[4] Nikolic VM, Perovic IM, Gavrilov NM, Pašti IA, Saponjic AB, Vulic PJ, et al. On the tungsten carbide synthesis for PEM fuel cell application - Problems, challenges and advantages. Int J Hydrogen Energy 2014;39:11175–85. https://doi.org/10.1016/J.IJHYDENE.2014.05.078.

[5] Wilberforce T, Khatib FN, Ijaodola OS, Ogungbemi E, El-Hassan Z, Durrant A, et al. Numerical modelling and CFD simulation of a polymer electrolyte membrane (PEM) fuel cell flow channel using an open pore cellular foam material. Sci Total Environ 2019;678:728–40.

https://doi.org/10.1016/J.SCITOTENV.2019.03.430.

[6] Jang D, Kim J, Kim D, Han WB, Kang S. Techno-economic analysis and Monte Carlo simulation of green hydrogen production technology through various water electrolysis technologies. Energy Convers Manag 2022;258:115499. https://doi.org/10.1016/J.ENCONMAN.2022.115499.

[7] Grid Stability Issues With Renewable Energy Sources, How They Can Be Solved. n.d. https://www.hivepower.tech/blog/grid-stability-issues-with-renewable-energy-how-they-can-be-solved (accessed May 15, 2022).

[8] Aneke M, Wang M. Energy storage technologies and real life applications – A state of the art review. Appl Energy 2016;179:350–77. https://doi.org/10.1016/J.APENERGY.2016.06.097.

[9] Puranen P, Kosonen A, Ahola J. Technical feasibility evaluation of a solar PV based off-grid domestic energy system with battery and hydrogen energy storage in northern climates. Sol Energy 2021;213:246–59. https://doi.org/10.1016/J.SOLENER.2020.10.089.

[10] Grey, blue, green – the many colours of hydrogen explained | World Economic Forum n.d. https://www.weforum.org/agenda/2021/07/clean-energy-green-hydrogen/ (accessed July 3, 2022).

[11] Energy density - Energy Education n.d. https://energyeducation.ca/encyclopedia/Energy_density (accessed May 18,

2022).

[12] International Energy Agency. The Future of Hydrogen: Seizing today's opportunities. IEA Publ 2019:203.

[13] Zhang F, Zhao P, Niu M, Maddy J. The survey of key technologies in hydrogen energy storage. Int J Hydrogen Energy 2016;41:14535–52. https://doi.org/10.1016/J.IJHYDENE.2016.05.293.

[14] North Cyprus News | Kib-Tek Summer Tariff Begins Today n.d. https://lgcnews.com/kib-tek-summer-tariff-begins-today/ (accessed July 9, 2022).

[15] The Solar Power Duck Curve Explained n.d. https://elements.visualcapitalist.com/the-solar-power-duck-curve-explained/ (accessed July 8, 2022).

[16] Escobar-Yonoff R, Maestre-Cambronel D, Charry S, Rincón-Montenegro A, Portnoy I. Performance assessment and economic perspectives of integrated PEM fuel cell and PEM electrolyzer for electric power generation. Heliyon 2021;7. https://doi.org/10.1016/J.HELIYON.2021.E06506.

[17] Fuel Cell Basics — Fuel Cell & Hydrogen Energy Association n.d. https://www.fchea.org/fuelcells (accessed July 6, 2022).

[18] Curtiss EM, Curtiss E. Electrical Grid Energy Storage Using Hydrogen: A

Feasibility Study. Macalester J Phys Astron 2021;9.

[19] Tashie-Lewis BC, Nnabuife SG. Hydrogen Production, Distribution, Storage and Power Conversion in a Hydrogen Economy - A Technology Review. Chem Eng J Adv 2021;8. https://doi.org/10.1016/J.CEJA.2021.100172.

[20] Greer M. U.S. Electric Markets, Structure, and Regulations. Electr Marg Cost Pricing 2012:39–100. https://doi.org/10.1016/B978-0-12-385134-5.00003-X.

[21] Distribution cooperative Definition | Law Insider n.d. https://www.lawinsider.com/dictionary/distribution-cooperative (accessed July 19, 2022).

[22] Cyprus Seasons n.d. https://www.cyprus-weather.com/article/cyprus-seasons.html (accessed August 1, 2022).

[23] Kktc elektrik kurumu 01 2022:6237.

[24] Pashaei A. Hydrogen production with water electrolysis method to use in fuel cell for electricity generation 2014. https://doi.org/10.13140/RG.2.1.3114.2565.

[25] Mazloomi K, Gomes C. Hydrogen as an energy carrier: Prospects and challenges. Renew Sustain Energy Rev 2012;16:3024–33. https://doi.org/10.1016/J.RSER.2012.02.028.

[26] Lee B, Heo J, Kim S, Sung C, Moon C, Moon S, et al. Economic feasibility studies of high pressure PEM water electrolysis for distributed H2 refueling stations. Energy Convers Manag 2018;162:139–44. https://doi.org/10.1016/J.ENCONMAN.2018.02.041.

[27] Step 6: Economic Feasibility | Nebraska Business Development Center | University of Nebraska Omaha n.d. https://www.unomaha.edu/nebraska-business-development-center/technology-commercialization/goldsmith-technology/step-6.php (accessed July 9, 2022).

[28] Science N, Division E. Economic Data and Modeling Support for the Two Regional Case Studies n.d.

[29] FOTW #1234, April 18, 2022: Volumetric Energy Density of Lithium-ion Batteries Increased by More than Eight Times Between 2008 and 2020 | Department of Energy n.d. https://www.energy.gov/eere/vehicles/articles/fotw-1234-april-18-2022-volumetric-energy-density-lithium-ion-batteries (accessed July 19, 2022).

[30] Law K, Rosenfeld J, Han V, Chan M, Chiang H, Leonard J. U.S. Department of Energy Hydrogen Storage Cost Analysis. US Dep Energy 2013:88.

[31] Stetson NT. Hydrogen Storage Program Area - Plenary Presentation - 2014.

[32] Ould Amrouche S, Rekioua D, Rekioua T, Bacha S. Overview of energy storage in renewable energy systems. Int J Hydrogen Energy 2016;41:20914–27.

https://doi.org/10.1016/J.IJHYDENE.2016.06.243.

[33] Shiva Kumar S, Himabindu V. Hydrogen production by PEM water electrolysis – A review. Mater Sci Energy Technol 2019;2:442–54. https://doi.org/10.1016/J.MSET.2019.03.002.

[34] Hydrogen Production: Electrolysis | Department of Energy n.d. https://www.energy.gov/eere/fuelcells/hydrogen-production-electrolysis (accessed July 7, 2022).

[35] INTRODUCTORY n.d.

[36] Chi J, Yu H. Water electrolysis based on renewable energy for hydrogen production. Cuihua Xuebao/Chinese J Catal 2018;39:390–4. https://doi.org/10.1016/S1872-2067(17)62949-8.

[37] Balat M. Potential importance of hydrogen as a future solution to environmental and transportation problems. Int J Hydrogen Energy 2008;33:4013–29. https://doi.org/10.1016/J.IJHYDENE.2008.05.047.

[38] Colella W, James B, Moron J, Saur G, Ramsden T. Techno-economic Analysis of PEM Electrolysis for Hydrogen Production. Electrolytic Hydrog Prod Work 2014:38.

[39] Gutiérrez-Martín F, Amodio L, Pagano M. Hydrogen production by water electrolysis and off-grid solar PV. Int J Hydrogen Energy 2021;46:29038–48.

https://doi.org/10.1016/J.IJHYDENE.2020.09.098.

[40] Miller E. II . 0 Hydrogen Production Sub-Program Overview. US Dep Energy 2016:17–23.

[41] Grigoriev SA, Porembsky VI, Fateev VN. Pure hydrogen production by PEM electrolysis for hydrogen energy. Int J Hydrogen Energy 2006;31:171–5. https://doi.org/10.1016/J.IJHYDENE.2005.04.038.

[42] FAQ | Nel Hydrogen n.d. https://nelhydrogen.com/faq/ (accessed July 7, 2022).

[43] d'Amore-Domenech R, Santiago Ó, Leo TJ. Multicriteria analysis of seawater electrolysis technologies for green hydrogen production at sea. Renew Sustain Energy Rev 2020;133. https://doi.org/10.1016/J.RSER.2020.110166.

[44] Sun F, Qin J, Wang Z, Yu M, Wu X, Sun X, et al. Energy-saving hydrogen production by chlorine-free hybrid seawater splitting coupling hydrazine degradation. Nat Commun 2021;12:1–11. https://doi.org/10.1038/s41467-021-24529-3.

[45] Atikol U, Aybar HS. Estimation of water production cost in the feasibility analysis of RO systems. Desalination 2005;184:253–8. https://doi.org/10.1016/J.DESAL.2005.02.065.

[46] Cengel YA. THERMODYNAMICS 9th edition. vol. 44. 2019.

[47] Petrecca G. Energy Conversion and Management. 2014. https://doi.org/10.1007/978-3-319-06560-1.

[48] Khotseng L. Fuel Cell Thermodynamics. Thermodyn Energy Eng 2019. https://doi.org/10.5772/INTECHOPEN.90141.

[49] Fuel Cells | Department of Energy n.d. https://www.energy.gov/eere/fuelcells/fuel-cells (accessed June 16, 2022).

[50] Larminie J, Dicks A. Fuel Cell Systems Explained Second Edition n.d.

[51] Sharma P, Pandey OP. Proton exchange membrane fuel cells: fundamentals, advanced technologies, and practical applications. PEM Fuel Cells 2022:1–24. https://doi.org/10.1016/B978-0-12-823708-3.00006-7.

[52] Sagar A, Chugh S, Sonkar K, Sharma A, Kjeang E. A computational analysis on the operational behaviour of open-cathode polymer electrolyte membrane fuel cells. Int J Hydrogen Energy 2020;45:34125–38. https://doi.org/10.1016/J.IJHYDENE.2020.09.133.

[53] Ohta T, Veziroglu TN. SA NE M SC PL O E – C EO AP LS TE S M SC PL O E – C EO n.d.;I.

[54] Ormerod RM. Solid oxide fuel cells. Chem Soc Rev 2003;32:17–28. https://doi.org/10.1039/B105764M.

[55] Jiang SP, Chen X. Chromium deposition and poisoning of cathodes of solid oxide fuel cells - A review. Int J Hydrogen Energy 2014;39:505–31. https://doi.org/10.1016/J.IJHYDENE.2013.10.042.

[56] Sakas G, Ibáñez-Rioja A, Ruuskanen V, Kosonen A, Ahola J, Bergmann O. Dynamic energy and mass balance model for an industrial alkaline water electrolyzer plant process. Int J Hydrogen Energy 2022;47:4328–45. https://doi.org/10.1016/J.IJHYDENE.2021.11.126.

[57] Ozden A, Shahgaldi S, Li X, Hamdullahpur F. A review of gas diffusion layers for proton exchange membrane fuel cells—With a focus on characteristics, characterization techniques, materials and designs. Prog Energy Combust Sci 2019;74:50–102. https://doi.org/10.1016/J.PECS.2019.05.002.

[58] Tu H, Stimming U. Advances, aging mechanisms and lifetime in solid-oxide fuel cells. J Power Sources 2004;127:284–93. https://doi.org/10.1016/J.JPOWSOUR.2003.09.025.

[59] Schuler JA, Wuillemin Z, Hessler-Wyser A, Comminges C, Steiner NY, Van Herle J. Cr-poisoning in (La,Sr)(Co,Fe)O 3 cathodes after 10,000 h SOFC stack testing. J Power Sources 2012;211:177–83. https://doi.org/10.1016/J.JPOWSOUR.2012.03.045.

[60] Malik V, Srivastava S, Bhatnagar MK, Vishnoi M. Comparative study and analysis between Solid Oxide Fuel Cells (SOFC) and Proton Exchange Membrane (PEM) fuel cell - A review. Mater Today Proc 2021;47:2270–5.

https://doi.org/10.1016/J.MATPR.2021.04.203.

[61] Fuel Cells : DOE Hydrogen Program n.d. https://www.hydrogen.energy.gov/fuel_cells.html (accessed July 3, 2022).

[62] Bushnell JB, Wolfram C. Ownership Change , Incentives and Plant Efficiency : The Divestiture of U . S . Electric Generation Plants. Univ Calif Energy Inst 2005.

[63] Jang H. Ownership, pricing, and productivity: the case of electric distribution cooperatives. Empir Econ 2019 592 2019;59:977–1001. https://doi.org/10.1007/S00181-019-01658-9.

[64] Greer ML. Can rural electric cooperatives survive in a restructured US electric market? An empirical analysis. Energy Econ 2003;25:487–508. https://doi.org/10.1016/S0140-9883(03)00050-1.

[65] Terzi R. Application of Exergy Analysis to Energy Systems. Appl Exergy 2018. https://doi.org/10.5772/intechopen.74433.

[66] Sevjidsuren G, Uyanga E, Bumaa B, Temujin E, Altantsog P, Sangaa D. Exergy Analysis of 1.2 kW NexaTM Fuel Cell Module. Clean Energy Better Environ 2012. https://doi.org/10.5772/50602.

[67] Mei B, Barnoon P, Toghraie D, Su CH, Nguyen HC, Khan A. Energy, exergy, environmental and economic analyzes (4E) and multi-objective optimization of

a PEM fuel cell equipped with coolant channels. Renew Sustain Energy Rev 2022;157. https://doi.org/10.1016/J.RSER.2021.112021.

[68] Dincer I, Rosen MA. Exergy Sustainable Development. 2012.

[69] Baschuk JJ, Li X. Mathematical model of a PEM fuel cell incorporating CO poisoning and O 2 (air) bleeding. Int J Glob Energy Issues 2003;20:245–76. https://doi.org/10.1504/IJGEI.2003.003966.

[70] Ahluwalia RK, Papadias DD, Peng J-K, Roh HS, Doe US, Washington DC. System Level Analysis of Hydrogen Storage Options Hydrogen and Fuel Cells Program 2020 Annual Merit Review and Peer Evaluation Meeting 2020:1–29.

[71] Zheng J, Liu X, Xu P, Liu P, Zhao Y, Yang J. Development of high pressure gaseous hydrogen storage technologies. Int J Hydrogen Energy 2012;37:1048–57. https://doi.org/10.1016/J.IJHYDENE.2011.02.125.

[72] Gravimetric energy density - Energy Education n.d. https://energyeducation.ca/encyclopedia/Gravimetric_energy_density (accessed July 19, 2022).

[73] Stationary Hydrogen Storage Applications - NPROXX n.d. https://nproxx.com/hydrogen-storage-transport/stationary-applications/ (accessed July 9, 2022).

[74] Çengel - Thermodynamics (An Engineering Approach) 8th Ed (TABELAS).pdf

- PDFCOFFEE.COM n.d. https://pdfcoffee.com/engel-thermodynamics-an-engineering-approach-8th-ed-tabelaspdf-2-pdf-free.html (accessed June 16, 2022).

[75] Example of demand side management / energy flexibility strategy with... | Download Scientific Diagram n.d. https://www.researchgate.net/figure/Example-of-demand-side-management-energy-flexibility-strategy-with-peak-shaving-valley_fig1_336931645 (accessed July 7, 2022).

[76] Sunrise and sunset in Cyprus n.d. https://www.worlddata.info/asia/cyprus/sunset.php (accessed July 9, 2022).

[77] Crystal Ball | Oracle n.d. https://www.oracle.com/applications/crystalball/ (accessed July 27, 2022).

[78] Zhang H, Lin G, Chen J. Evaluation and calculation on the efficiency of a water electrolysis system for hydrogen production. Int J Hydrogen Energy 2010;35:10851–8. https://doi.org/10.1016/J.IJHYDENE.2010.07.088.

[79] Bin C, Hajimolana YS, Venkataraman V, Ni M, Aravind P V. Integration of Reversible Solid Oxide Cells with methane synthesis (ReSOC-MS) in grid stabilization. Energy Procedia 2019;158:2077–84. https://doi.org/10.1016/J.EGYPRO.2019.01.479.

[80] Reynolds WC, Perkins HC (Henry C. Engineering thermodynamics 1977:690.

[81] Ay M, Midilli A, Dincer I. Exergetic performance analysis of a PEM fuel cell. Int J Energy Res 2006;30:307–21. https://doi.org/10.1002/er.1150.

[82] Al C. Appendix: Standard Chemical Exergy. Thermodyn Destr Resour 2011:489–94. https://doi.org/10.1017/cbo9780511976049.024.

[83] PEM-FCS Stack Technology | Nedstack n.d. https://nedstack.com/en/pem-fcs-stack-technology (accessed July 8, 2022).

[84] 40.40 - Economic Feasibility Study n.d. https://ofm.wa.gov/sites/default/files/public/legacy/policy/40.40.htm (accessed July 9, 2022).

[85] What is the Savings-to-Investment Ratio (SIR)? - Colorado C-PACE n.d. https://copace.com/faq/what-is-the-savings-to-investment-ratio-sir/ (accessed July 9, 2022).

[86] الوزير غج, الشعراني إف. No Title. التعويضات المتحركة الكاملة و التعويضات الفكية الوجهية. منشورات جامعة دمشق 2006;1:1999–6.

[87] Kato T, Kubota M, Kobayashi N, Suzuoki Y. Effective utilization of by-product oxygen from electrolysis hydrogen production. Energy 2005;30:2580–95. https://doi.org/10.1016/j.energy.2004.07.004.

[88] Hydrogen Storage - Basics | Department of Energy n.d. https://www.energy.gov/eere/fuelcells/hydrogen-storage-basics-0 (accessed

March 17, 2022).

[89] (8) Hossein Nami n.d. https://www.researchgate.net/profile/Hossein-Nami (accessed July 30, 2022).

[90] (1) (PDF) Exergy analysis of a natural gas fired combined cycle power generation unit n.d. https://www.researchgate.net/publication/245402170_Exergy_analysis_of_a_natural_gas_fired_combined_cycle_power_generation_unit (accessed July 31, 2022).

[91] Curtiss EM, Curtiss E. Electrical Grid Energy Storage Using Hydrogen: A Feasibility Study. Macalester J Phys Astron 2021;9.

[92] Powerwall | Tesla n.d. https://www.tesla.com/powerwall (accessed August 4, 2022).

[93] Used Lithium-Ion Batteries | US EPA n.d. https://www.epa.gov/recycle/used-lithium-ion-batteries (accessed August 4, 2022).

[94] Sales of electric heaters soar in Germany amid winter gas crisis fears | Euronews n.d. https://www.euronews.com/2022/08/03/sales-of-electric-heaters-soar-in-germany-amid-winter-gas-crisis-fears (accessed August 9, 2022).

[95] Germany’s power system weathers heat wave despite fossil plant curbs | Clean Energy Wire n.d. https://www.cleanenergywire.org/news/germanys-power-

system-weathers-heat-wave-despite-fossil-plant-curbs (accessed August 9, 2022).

[96] Epex Spot: Europe Power Prices Set to Climb Even Higher After Record Month - Bloomberg n.d. https://www.bloomberg.com/news/articles/2022-07-29/europe-power-prices-set-to-climb-even-higher-after-record-month (accessed August 9, 2022).

[97] Germany’s Energy Catastrophe n.d. https://quillette.com/2022/07/14/germanys-energy-catastrophe/ (accessed August 9, 2022).